UNIVERSIDADE ESTADUAL DE CAMPINAS

Heloisa Helena Mithie Della Colleta

Conteúdo, biossíntese e degradação de ácido hialurônico na próstata ventral de ratos: Efeito da castração e papel das células musculares lisas

Tese apresentada ao Instituto de Biologia para obtenção do Título de Doutor em Biologia Celular e Estrutural na área de Biologia Celular.

Orientador: Prof. Dr. Hernandes Faustino de Carvalho

FICHA CATALOGRÁFICA ELABORADA PELA
BIBLIOTECA DO INSTITUTO DE BIOLOGIA – UNICAMP

D38c

Della Colleta, Heloisa Helena Mithie
Conteúdo, biossíntese e degradação de ácido hialurônico na próstrata ventral de ratos: efeito da castração e papel das células musculares lisas / Heloísa Helena Mithie Della Colleta. -- Campinas, SP: [s.n.], 2005.

Orientador: Hernandes Faustino de Carvalho
Tese (Doutorado) – Universidade Estadual de Campinas. Instituto de Biologia.

1. Próstata. 2. Ácido hialurônico. 3. Castração. 4. Célula muscular lisa. 5. Real-time PCR. I. Hernandes Faustino de Carvalho. II. Universidade Estadual de Campinas. Instituto de Biologia. III. Título.

Campinas, 28 de fevereiro de 2005.

Banca Examinadora

Prof. Dr. Hernandes F Carvalho (orientador) _____ (Assinatura)

Prof. Dr. Sebastião Roberto Taboga _____ (Assinatura)

Prof. Dr. Sérgio Luis Felisbino _____ (Assinatura)

Profa. Dra. Christine Hackel _____ (Assinatura)

Profa. Dra. Carmen Veríssima Ferreira _____ (Assinatura)

Prof. Dr. Paulo Pinto Joazeiro _____ (Assinatura)

Profa. Dra. Laurecir Gomes _____ (Assinatura)

Dedicatória

Só há uma pessoa a quem dedicar esta tese: Hernandes.

Para começar a dedicatória, fui buscar duas definições: ORIENTAR, que é *reconhecer a situação, estudar as diversas circunstâncias para assim regular a sua conduta, o seu modo de proceder*. Em seguida, como não poderia deixar de ser, foi CONFIANÇA, definida como *convicção íntima acerca da probidade, diligência, talento ou discrição de alguém.*

Nenhuma pessoa, durante estes anos, teve mais confiança em mim do que você. Além disso, existe ainda o fato de você ter acreditado na minha capacidade. Acho que em muitas situações você acreditou mais em mim do que eu mesma seja para realizar algumas metodologias, seja apenas para apresentar um seminário de grupo de um dia para o outro. Em alguns momentos houveram descompassos, que acredito não terem maculado o que se foi criado. Tudo o que se tem aqui nesta tese e mais uma grande parte que está no meu íntimo deve-se a você, a pessoa que me orientou.

Profissionalmente amadureci muito e sem sombra de dúvida existe uma enorme contribuição sua. Maneiras de pensar, condutas, cobranças, formas de se colocar as idéias, ser objetiva... Pode ser (e tenho certeza disso) que muitas coisas ainda faltam, mas há uma nítida diferença do profissional que eu sou hoje do profissional que eu era antes de iniciar meu doutorado no seu laboratório.

Depois destes anos em seu convívio, só tenho que te agradecer. Muito obrigada por disponibilizar seu laboratório e seus equipamentos, por me ajudar a analisar os resultados e escrever os artigos, por permitir meu crescimento profissional. Espero que de alguma forma eu tenha retribuído parte disso tudo.

Mais uma vez, obrigada pela orientação, confiança e credibilidade.

Esta tese é sua...

Agradecimentos

Ao Prof. Dr. Hernandes F Carvalho por me orientar neste trabalho, mas principalmente por confiar em mim na execução de todos os experimentos. Nunca vou esquecer da credibilidade que em mim foi depositada, além da oportunidade de ampliar minha mente para o meu amadurecimento profissional.

Ao Prof. Dr. Sérgio Luís Felisbino por constantemente colaborar na execução deste trabalho, desde a realização de experimentos até a leitura da versão final da tese e participação da banca examinadora. Senti muito a sua falta quando você foi embora, mas logo percebi que a distância física não era um problema. A sua amizade e o seu coleguismo no trabalho foram (e continuaram sendo) muito importantes para mim.

Ao Prof. Dr. Sebastião Roberto Taboga por estar presente em todos os meus momentos acadêmicos, auxiliando nas bancas e sempre apresentando colocações pertinentes. O que mais admiro em você é acapacidade que você tem de fazer estas colocações de forma agradável. Imagino que isso seja um dom, mas um dom que nós podemos adquirir e assim vou tentar ser. Obrigada por me apresentar este exemplo de profissional.

Ao Prof. Dr. Paulo Pinto Joazeiro que também esteve sempre presente nestes anos de doutorado, participando das bancas, auxiliando na aquisição de imagens, lendo cuidadosamente minha tese e sempre apresentando sugestões. Suas observações sempre me foram muito importantes, até o último momento, quando fizemos a pré-banca e, dentre os assuntos de tese, você me contou do início do seu pós-doutorado na França. Fico extremamente agradecida pela sua dedicação aos meus manuscritos.

À Profa. Dra. Christine Hackel por aceitar compor a banca examinadora desta tese e também por disponibilizar seus conhecimentos e seu laboratório para que eu pudesse dar os primeiros passos no RT-PCR. A sua disponibilidade e amabilidade me foram muito úteis.

À Profa. Dra. Carmen Veríssima Ferreira por aceitar prontamente compor a banca examinadora desta tese e desta forma, poder contribuir em mais esta etapa da minha vida acadêmica.

Aos meus companheiros de jornada diária no laboratório agradeço pelo fato de todos tentarmos, de uma forma ou de outra, manter o bom relacionamento, que eu acredito ser a marca do laboratório. Pelas minhas contas, convivi com 21 pessoas desde o primeiro dia que cheguei, e por isso não citarei um a um. No entanto, cada um de vocês teve importante participação nestes anos em que convivemos. Cada um de vocês, em suas respectivas particularidades, ensinou-me um pouco, seja na profissão, seja na vida. Tenham certeza de que levarei vocês comigo, onde quer que nós estejamos e que, de onde eu estiver, estarei sempre à disposição, para o que vocês precisarem.

À Eliane Antonioli, que colaborou comigo em um dos artigos apresentados nesta tese. A sua garra, a sua competência e a sua coragem são exemplos para mim. Nossas conversas foram sempre muito esclarecedoras. O fato de termos artigos em conjunto é um motivo de orgulho para mim. Estarei torcendo muito por você, sempre.

À Líliam, por estar sempre atenta aos prazos, assinaturas de documentos, mas principalmente por cuidar de mim nestes procedimentos finais. Sem a sua preocupação talvez eu não tivesse conseguido entregar tudo no prazo. Muito, muito obrigada. A sua presteza é a sua marca.

À Bia, por ter correspondido a todos os meus pedidos e por cuidar de todos os documentos necessários.

Às professoras Dra. Shirlei Pimentel e Dra. Maria Júlia Marques por estarem sempre dispostas a sanar as dúvidas e por se empenharem em fazer o Curso de Pós-Graduação ser um dos melhores do país.

Ao Prof. Dr. Domingos da Silva Leite por ceder seu laboratório e equipamentos para a realização de alguns experimentos o que, acima de tudo, permitiu a manutenção do nosso contato. Tenha certeza de que nunca me esquecerei que os primeiros ensinamentos dentro de um laboratório foram dados por você.

À Profa. Dra. Maria Sílvia Viccari Gatti, por ceder alguns de seus equipamentos, que colaboraram na execução deste trabalho. A sua contribuição, não só nesta tese, é muito importante para mim. Sei que de perto ou de longe, você sempre olhou por mim.

À Profa. Dra. Sara T Saad por permitir a realização do Real-Time PCR, que contribuíram para a obtenção de resultados muito importantes para o trabalho. Agradeço em especial a Adriana Duarte e ao Samuel Medina por me auxiliarem na execução dos experimentos.

À Daniela Cabral, juntamente com sua orientadora Profa. Dra. Christine Hackel, por me ensinarem os primeiros passos com o RT-PCR.

Aos amigos de Botucatu Luís Justulin, Raquel, Virgínia, Robson, Danilo, Francis, Rodrigo e Michele, entre outros, por me receberem muito bem e terem feito meus dias em Botucatu serem extremamente agradáveis. O *meeting* de quinta é algo maravilhoso.

Ao meu querido amigo Ricardo por ter me hospedado nas vezes que precisei ir a Botucatu. Obrigada por me receber prontamente todas as vezes que precisei. A sua hospitalidade está relacionada a alguns destes resultados.

Aos meus queridos amigos Mário Paulo, Gleize, Rosabel, Sílvia Simi, Cleide, Luciano e Márcia Tommy que souberam entender minha decisão de "abandonar-lhes", apoiaram-me sem questionar e mantiveram a nossa amizade. Vocês serão sempre especiais para mim.

Aos meus queridos amigos da turma 90 e agregados, presença sempre tão importante na minha vida. Sei que torcemos muito uns pelos outros e isso é muito importante para todos nós. O pensamento positivo de qualquer parte do mundo funciona!!!

À Fundação de Amparo à Pesquisa do Estado de São Paulo (FAPESP) e à Coordenação de Aperfeiçoamento de Pessoal de Ensino Superior (CAPES) por terem me concedido auxílio financeiro para o desenvolvimento deste trabalho.

Sumário

Resumo 10

Abstract 12

Introdução 15

O ácido hialurônico, suas sintases, as hialuronidases e as hialaderinas 15

A próstata 24

Considerações gerais 30

Objetivos 33

Artigo 1 – Effects of castration on hyaluronan synthesis and degradation in the rat ventral prostate 36

Artigo 2 – Culturing rat prostatic smooth muscle cells: Maintenance of the differentiated state and hyaluronan synthesis 65

Conclusões Gerais 86

Referências Bibliográficas 88

RESUMO

O hialuronam (ou ácido hialurônico, AH) é um importante componente do espaço matricelular, estando presente tanto na matriz extracelular, como na superfície das células. Suas funções são variadas, mas estão sempre associadas à criação de um espaço pouco denso e extremamente hidratado, permitindo a proliferação e migração celular, típicas de processos como a embriogênese, cicatrização e invasão tumoral. Neste trabalho foi desenvolvido um estudo do metabolismo do ácido hialurônico na próstata ventral de ratos. Numa primeira etapa foi verificado o efeito da castração por 7, 14 e 21 dias sobre o conteúdo e distribuição do AH, assim como uma avaliação do papel da HA sintase 2 (HAS2) e da hialuronidase 1 (Hyal1). Para tanto, foram empregados ensaios de marcação tecidual de AH com a utilização de sonda marcada com fluoresceína, quantificação de AH por ensaio competitivo, determinação dos tamanhos das cadeias de AH por cromatografia em gel filtração, determinação dos níveis de expressão das enzimas HAS2 e Hyal1 por Real Time PCR, localização desta expressão por hibridação *in situ* e localização do receptor CD44 por imunohistoquímica. Na segunda etapa, foram estudadas células musculares lisas (CML) isoladas de ratos e mantidas em cultura, quanto à expressão de marcadores da diferenciação deste tipo celular e quanto à produção de AH, utilizando imunocitoquímica e RT-PCR para marcadores de CML, imunocitoquímica para o receptor CD44, quantificação de AH por ensaio competitivo e por medida de área de *coat*. Os resultados demonstram que o AH é encontrado tanto no epitélio quanto no estroma prostático e que há uma redução no conteúdo total de AH na próstata ventral, com um predomínio de cadeias curtas. Além disto, foi verificado que estas modificações são, ao menos em parte, devidas à manutenção da expressão da HAS2 e um aumento na expressão da Hyal1. Foi observado também, por outro lado, que ocorre uma diminuição na atividade da hialuronidase lisossomal. Experimentos de hibridação *in situ* demonstraram a presença da HAS2 no epitélio e em diversas células do estroma, com exceção das células musculares lisas e endoteliais. Com a castração, a expressão da HAS2 e da Hyal1 aumenta no estroma. Foi demonstrado também que as células musculares lisas prostáticas de rato em cultura mantêm a expressão de marcadores da diferenciação (smoothelin, SM22 e calponina) e que esta expressão não foi

dependente de insulina nem testosterona. A concentração de ácido hialurônico no meio de cultura variou nas diferentes passagens (0-8), assim como variou o tamanho do *coat* ao redor das células. Surpreendentemente, nas passagens 3 e 4 houve uma queda brusca na síntese de HA. Os resultados demonstram uma modificação no padrão expressão e de distribuição do ácido hialurônico na próstata ventral de ratos, com o comprometimento de diversos tipos celulares, que resultam na diminuição do conteúdo total. Conclui-se também que células musculares lisas em cultura mantêm-se diferenciadas e que são capazes de sintetizar e formar um *coat* na sua superfície.

ABSTRACT

Hyaluronan (or hyaluronic acid, HA) is an important component of the matricellular space. It is found in both extracelular matrix and at the cell surface. It has many functions, but is always associated with the establishment of a looser and hydrated space, allowing the cells to proliferate and migrate, in processes such as embryogenesis, healing and tumor invasion. In this work, we have studied some aspects of HA metabolism in the rat ventral prostate. In a firt series of experiments, the effect of castration for 7, 14 and 21 days on the content and distribution of HA, as well as an evaluation of the function of HA synthase 2 (HAS2) and hyaluronidase 1 (Hyal1). For this, were done tecidual HA localization with fluorescein probe, measurement of HA content in a competitive binding assay, determination of HA chain size variation using gel filtration cromatography, determination of expression levels of HAS2 and Hyal1 enzymes by Real Time PCR, localization of these expression by *in situ* hybridization and CD44 localization by immunohistochemistry. In a second series of experiments, the rat prostatic smooth muscle cells (SMC) were isolated and maintained *in vitro* for the study of the expression of molecular markers of the differentiated state and of the production of HA, using immunohistochemistry e RT-PCR for SMC markers, immunocitochemistry for CD44 receptor, HA quantification by competitive binding assay and measurement of coat area. The results demonstrate that HA is found in both epithelium and stroma and that there is a decrease in the total amount of HA in the organ after castration, with a predominance of short chains. Besides, it was observed that these modifications are, at least in part, due to a sustained expression of HAS2 and an increased expression of Hyal1. On the other hand, a reduction in lysosomal hyaluronidase activity was also observed. *In situ* hybridization showed the presence of HAS2 mRNA in both epithelium and stroma. Different stromal cells, with the exception of SMC and endothelial cells, expressed HAS2. Castration resulted in increased expression of HAS2 and Hyal1 in the stroma. It was also demonstrated that SMC kept in culture express the differentiation markers smoothelin, SM22 and calponin and that this expression pattern was not dependent on either insulin or testosterone. The concentration of HA in the culture medium and the size of the cell coat varied as cells were subcultured through passages 0-8. Surprisingly, a

severe drop in HA synthesis was observed at passages 3 and 4. The results demonstrate a modification in the pattern of expression and distribution of HA in the rat ventral prostate in response to castration, and the involvement of different cell types in the decreasing amount of HA. It is also concluded that SMC preserve the differentiated state in culture and that they are able to assemble a HA coat.

Introdução

O ácido hialurônico, suas sintases, as hialuronidases e as hialaderinas

Ácido hialurônico (AH) é um polissacarídeo da família dos glicosaminoglicanos (GAGs) que foi isolado pela primeira vez a partir do corpo vítreo de bovinos (Meyer & Palmer, 1934). A primeira descrição da estrutura química da molécula foi realizada em 1954 por Weissman & Meyer, quando foi demonstrado que o ácido hialurônico é composto por unidades repetitivas de dissacarídeos de ácido urônico e de um açúcar aminado, na forma de ácido D-glicurônico e de D-N-acetilglicosamina, ligados entre si entre as pontes glicosídicas beta-1,4 e beta-1,3 que se alternam. A estrutura química do dissacarídeo formado é energeticamente estável, uma vez que as hidroxilas, a carboxila e o carbono anomérico adjacente ao açúcar estão em posições equatoriais estericamente favoráveis, enquanto todos os átomos de hidrogênio ocupam uma posição axial estericamente menos favorável (Fig. 1).

Diferentemente de outros glicosaminoglicanos que são sulfatados, o AH é carboxilado e não se associa covalentemente à proteínas na formação de proteoglicanos.

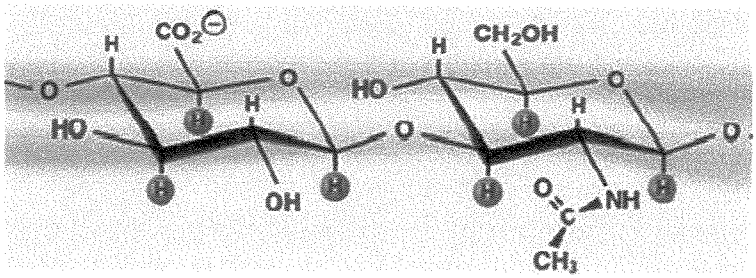

Figura 1. Estrutura química do dissacarídeo que se repete na composição da molécula de ácido hialurônico. A metade da esquerda representa o ácido glicurônio β 1-3 e a da direita, o N-acetilglicosamina β 1-4. As moléculas de hidrogênio circundadas em rosa contribuem para a baixa hidrofobicidade da molécula.

Quanto à estrutura que o ácido hialurônico adquire em solução fisiológica, foi observado que ocorrem pontes de hidrogênio internas entre os dissacarídeos, compondo uma estrutura terciária em forma de fita, com uma face não-polar hidrofóbica e uma face polar hidrofílica. Esta estrutura traz conseqüências importantes, já que pequenas moléculas como água, eletrólitos e nutrientes podem difundir-se livremente através dela, enquanto moléculas grandes, como proteínas, são excluídas devido ao tamanho hidrodinâmico que apresentam em solução. A presença de cargas negativas contribui para que o AH crie um ambiente altamente hidratado.

Os glicosaminoglicanos que formam proteoglicanos são sintetizados e modificados no retículo endoplasmático rugoso e no complexo de Golgi, sendo secretados de forma semelhante às outras glicoproteínas. O AH, por sua vez, é sintetizado como um polissacarídeo, já em sua forma final, por enzimas que estão localizadas na membrana plasmática, chamadas ácido hialurônico sintase (HAS - *hyaluronan synthase*) (Prehm, 1984). Até o momento, foram descritas três isoformas da HAS em humanos: HAS1 (Shyjan et al., 1996), HAS2 (Watanabe & Yamaguchi, 1996) e HAS3 (Spicer et al., 1997) e seus genes ortólogos foram identificados em camundongos e ratos. Embora sejam codificados por genes distintos, os produtos protéicos das HAS apresentam seqüências de aminoácidos e características estruturais moleculares muito similares.

A HAS cataliza polímeros lineares e longos através da adição repetitiva de ácido glicurônico e N-acetilglicosamina para a elongação da cadeia. O número de repetições dissacarídicas pode chegar a mais de 10.000, o que representa uma massa molecular de aproximadamente 4 milhões de Daltons (considerando-se que cada dissacarídeo apresenta aproximadamente 400 Da). O comprimento médio de um dissacarídeo é de cerca de 1 nm e, sendo assim, uma molécula de AH com 10.000 repetições dissacarídicas pode atingir um comprimento de 10 μm, o que representa o diâmetro de um eritrócito (Hascall & Laurent, 1997).

Inicialmente acreditava-se que a translocação do AH para o meio extracelular ocorria à medida que os açúcares eram adicionados à cadeia de AH, pela própria HAS, que estaria associada a um conjunto de 14-18 moléculas do fosfolipídio cardiolipina (Tlapak-Simmons et al., 1998). A importância da cardiolipina para a atividade da HAS foi

comprovada após a purificação da HAS que, sem a cardiolipina, apresentava baixa atividade de síntese de AH. Após a adição de cardiolipina, a atividade enzimática aumentava em cerca de 10 vezes (Tlapak-Simmons et al.1999a, b).

A organização da HAS na membrana plasmática parece ser semelhante em bactérias e em células eucarióticas. No modelo proposto para estreptococos, a enzima está alocada na membrana plasmática, atravessa a bicamada lipídica quatro vezes e apresenta dois domínios de associação à membrana (que não atravessam a bicamada) (Fig. 2). Nas células eucarióticas, existe mais um domínio extracelular, aumentando, assim, para 6 o número de domínios que atravessam a bicamada lipídica (Weigel et al., 1997). A maior parte da proteína (cerca de 60%) está na porção intracelular, incluindo as regiões N e C-terminal. Mais recentemente, Heldermon et al. (2001) descreveram que, em *Streptococcus pyogenes*, há seis organizações possíveis da HAS na membrana da bactéria. As diferenças ocorrem segundo a hidrofobicidade da proteína. A Fig. 2 mostra uma representação esquemática da organização da HAS na membrana das células de estreptococos.

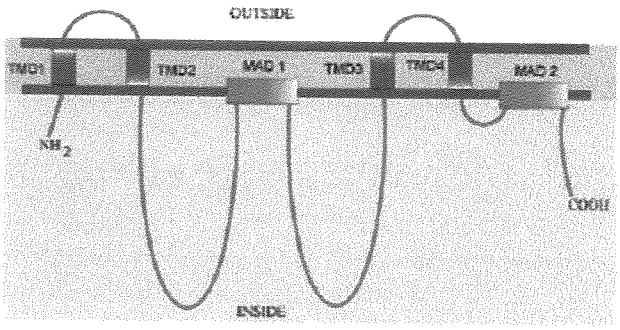

Figura 2. Representação esquemática da organização da HAS na membrana de estreptococos Organização da HAS na membrana de estreptococo. Note que a grande maioria da proteína está no meio intracelular, incluindo os domínios N e C-terminal. Existem dois tipos de domínios na membrana: os que atravessam a membrana (TMD), representados em vermelho, e os domínios que apenas estão em contato com a membrana (MAD), representados em verde. Reproduzido de www.glycoforum.com.

Estudos das propriedades enzimáticas das três isoformas das HAS demonstraram que em cultura de células clonadas com os genes das HAS, a HAS1 forma uma capa

pericelular de AH significativamente menor do que as capas de AH formadas pelas HAS2 e HAS3, sugerindo que propriedades enzimáticas intrínsecas das três HAS podem regular o tamanho da capa de AH (Itano et al., 1999a). Além disso, foi observado que as cadeias de AH formadas pelas HAS1 e HAS2 ($2x10^5$ a $\sim 2x10^6$) são ligeiramente maiores do que as cadeias formadas pelas HAS 3 ($1x10^5$ a $1x10^6$). As avaliações da cinética enzimática demonstraram que as três HAS são distintas com relação à estabilidade enzimática, ao índice de elongação de AH e para os valores aparentes de K*m* para os dois substratos (UDP-GlcNAc e UDP-GlcUA) da cadeia de AH (Itano et al., 1999a). Brinck & Heldin (1999) também fizeram a transfecção das três HAS em células CHO e verificaram que a HAS1 apresentava uma capacidade de síntese de AH de 4 a 10 vezes menor do que as HAS2 e HAS3 e que o tamanho da cadeia de AH sintetizada pelas células e pelos extratos de membrana variavam consideravelmente entre elas.

Recentemente, Prehm & Schumacher (2004) demonstraram que algumas drogas capazes de bloquear transportadores ABC (ATP *Binding Cassettes*) inibem a produção de AH em fibroblastos *in vitro* e sugeriram que MRP5 (um membro da família dos transportadores ABC) é o principal transportador do AH em fibroblastos humanos. Em *Streptococcus pyogenes*, que tem como principal fator de virulência a cápsula de AH (Husmann et al., 1997; Wessels et al., 1991), foi verificado que o transportador ABC é responsável pela exportação do AH e que seu gene é localizado nas adjacências do gene da HAS, em direção oposta no quadro aberto de leitura (ORF - *open reading frame*) (Ouskova et al., 2004).

Já em 1950, Karl Meyer detectou a degradação enzimática do AH e denominou a enzima responsável por esta degradação como hialuronidase. Meyer descreveu três tipos de hialuronidases, classificadas de acordo com análises bioquímicas das enzimas e de seus produtos de reação:

1. Hialuronidases encontradas em mamíferos, que são endo-beta-N-acetilhexosaminidases e que têm como principais produtos tetrassacarídeos e hexassacarídeos. As hialuronidases de mamíferos possuem tanto atividade hidrolítica como de transglicosidase e podem degradar além do AH, condroitim sulfato e, em menor especificidade, dermatam sulfato.

2. Hialuronidases bacterianas também são endo-beta-N-acetilhexosaminidases, mas possuem atividade de β-eliminação e reduzem a cadeia de AH a dissacarídeos.
3. Hialuronidases encontradas em sanguessugas, parasitas e crustáceos, são endo-beta-glicuronidases que geram tetrassacarídeos e hexassacarídeos.

Em humanos as hialuronidases são denominadas Hyal ou PH-20. Foram encontrados até o momento sete genes que codificam hialuronidases e que estão agrupados nos cromossomos 3p21.3 (*HYAL1*, *HYAL2*, *HYAL3*) e 7q31.3 (*HYAL4*, *PH-20/SPAM1*, *HYALP1*) (Csóka et al., 1999). No entanto, não foram encontradas evidências de expressão protéica do gene *HYALP1*, que, desta forma, é considerado, ao menos no homem, um pseudo-gene; já em camundongos, possivelmente este gene tenha significado funcional (Csóka et al., 2001). O sétimo gene, embora esteja associado ao conjunto de hialuronidases, é considerado ainda um codificador de uma provável hialuronidase, que não está relacionado aos outros seis genes e é encontrado no cromossomo 10q24 (Heckel et al., 1998). A enzima produzida por este gene é imunologicamente semelhante às hialuronidases que ocorrem em meningiomas, porém ainda não está claro se esta atividade está relacionada à degradação do AH. Há evidência de que uma variante deste gene produz uma proteína com atividade β-N-acetilglicosaminidase (Comtesse et al., 2001).

As hialuronidases são encontradas em vários tecidos e organismos, com uma grande especificidade pelo tecido e uma ampla variação de pH ótimo. Nos vertebrados, as hialuronidases podem ser divididas em dois grupos: as de atividade neutra, como a PH-20 (Primakoff et al., 1985; Lin et al., 1994) e aquelas com pH ótimo ácido, como as encontradas no fígado (Gold, 1982) e no plasma (De Salegui & Pigman, 1967).

Apesar do reconhecimento da atividade hialuronidásica, as dificuldades em se purificar e caracterizar estas enzimas comprometeram o conhecimento aprofundado das características bioquímicas e moleculares destas enzimas. Deste modo, somente em 1997 Frost e colaboradores obtiveram os primeiros resultados de caracterização da Hyal-1. Até o momento, as enzimas mais estudadas são Hyal-1 e a Hyal-2, sendo que a Hyal-1 é a mais abundante por ser encontrada no plasma e na urina. A Hyal-2, por sua vez, está localizada na membrana plasmática dos lisossomos, embora seja também encontrada em pequenas quantidades na forma solúvel. Provavelmente a Hyal2 seja a mais importante de todas as

hialuronidases, já que camundongos *knock out* para o gene da Hyal-2 não se desenvolvem (Stern, 2003). A Hyal-3 é amplamente expressa, mas sua atividade não é detectada facilmente. Possivelmente, há uma expressão coordenada entre Hyal-2 e Hyal-3, que são reguladas por citocinas inflamatórias como IL-1 e TNF-α, enquanto a expressão de Hyal-1 parece não ser afetada pelas citocinas (Flannery et al., 1998). A PH-20 é uma hialuronidase encontrada na membrana acrossomal do espermatozóide e que participa do processo de fertilização, por facilitar a penetração do espermatozóide no óvulo (Cherr et al., 2001).

As hialuronidases de vertebrados ocorrem em uma variedade de formas oriundas de diferenças no processamento pós-traducional. No entanto, não é possível determinar os papéis específicos destas isoformas nos processos de catabolismo, bem como determinar a especificidade tecidual de cada isoenzima. Isso indica que os modelos de catabolismo de AH, em sua maioria, são hipotéticos (Stern, 2003).

O *turnover* do AH nos mamíferos em situação normal é surpreendentemente alto quando comparado a outros componentes de matriz extracelular. Na pele, onde se concentra cerca de 50% do AH corporal, a meia-vida do AH é de cerca de 24 horas; em tecidos aparentemente inertes, como cartilagem, a meia-vida do AH é de uma a três semanas e na corrente sanguínea, a meia-vida é de dois a cinco minutos (Stern & Csóka, 2000). O catabolismo do AH envolve sua internalização, o que pode explicar, em parte a presença do AH intracelular (outra explicação é o fato do transportador ABC não estar ativo, como descrito acima). Tammi e colaboradores (2001) descreveram uma via de entrada do AH para o interior de queratinócitos em cultura e comprovaram que a degradação do AH ocorre nos lisossomos.

Desde a década de 40, têm sido descritos alguns inibidores de hialuronidases circulantes (Haas, 1946; Dorfman et al., 1948; Moore & Harris, 1949). Foi verificado que estes inibidores eram glicoproteínas termolábeis de alta massa molecular (Newman et al., 1955), que podiam (Mathews & Dorfman, 1955) ou não (Fiszer-Szafarz, 1968) necessitar da presença de magnésio para a sua atividade. Poucos estudos foram realizados com estes inibidores de hialuronidases, porém Mio e colaboradores (2000) evidenciaram que um membro da família de inibidores inter-α I seria o responsável pela atividade inibitória das

hialuronidases. Uma revisão a respeito dos inibidores de hialuronidases pode ser encontrada em Mio & Stern (2002).

O AH interage com proteínas, que podem ou não ser classificadas como receptores para AH. As proteínas que se ligam ao AH recebem a nomenclatura de hialaderinas e são divididas de acordo com a sua localização (na matriz extracelular, na superfície celular ou intracelularmente) e de acordo com as seqüências capazes de se ligar ao AH. A Fig. 3 mostra a diversidade do grupo das hialaderinas, classificadas de acordo com a sua localização.

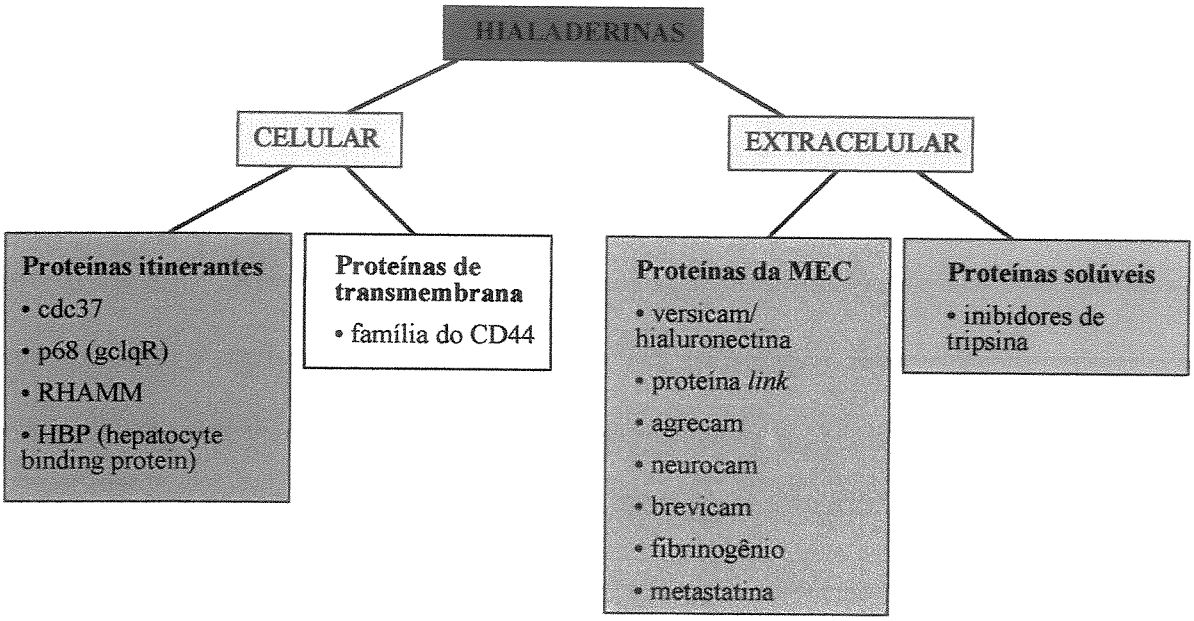

Figura 3. Principais hialaderinas descritas, classificadas de acordo com as suas localizações.

A grande maioria das hialaderinas liga-se ao AH via 100 aminoácidos básicos, conhecidos como módulo de ligação ou "módulo *link*", diferenciando-se uma das outras pela porção na qual ocorre a ligação com o AH.

Das hialaderinas celulares, algumas são chamadas de itinerantes, por serem encontradas tanto na superfície celular, como na porção interna das células.

Do grupo das hialaderinas, a família do CD44 é a mais conhecida e estudada e é designada como "a família dos receptores para AH", embora outras proteínas também desempenhem papel de receptor para AH.

O CD44 está envolvido em uma ampla variedade de funções celulares como migração celular, agregação célula-célula, retenção de matriz pericelular e sinalização matriz-célula e célula-matriz. Em 2001, Tammi e colaboradores descreveram a função do CD44 no catabolismo do AH.

O AH pode ser retido na superfície das células em cultura através do receptor CD44. A partir de um ensaio de exclusão de partículas em cultura de condrócitos, após a adição de hemácias fixadas, foi possível observar um halo ao redor das células, denominado *coat*. Quando as células foram incubadas com um anticorpo que inibia a ação do CD44, não houve mais a formação de um halo pericelular. O tratamento com hialuronidase, da mesma forma, inibiu a formação de capa pericelular. Deste modo, foi possível constatar que era o AH que estava retido ao redor das células e que o CD44 era responsável por esta retenção.

Uma outra forma de retenção de AH ao redor das células é através da ligação com a própria enzima que sintetiza o AH, a HAS. Em alguns ensaios *in vitro* verificou-se que mesmo após a incubação das células com o anticorpo que inibe a atividade do CD44 continuava ocorrendo a retenção de AH ao redor da célula. A Fig. 4 mostra o modo pelo qual o AH pode se associar à célula e um ensaio de exclusão de partícula, onde é possível observar a formação de um halo ao redor da célula.

Há muita discussão a respeito do tamanho da cadeia de AH formada e suas relações com as funções desempenhadas no tecido. Em vertebrados, o AH está envolvido em processos de desenvolvimento embrionário, migração celular e sinalização (Tammi et al., 2002). Muitos dos processos de transdução de sinais envolvem a ligação do AH com as hialaderinas (Turley et al., 2002), comprovando que o AH é muito mais do que uma simples molécula de preenchimento de espaço. Estudos têm demonstrado que o tamanho da cadeia de AH pode determinar as funções biológicas que serão desempenhadas pelo AH (Camenisch et al., 2000, Toole et al., 2002).

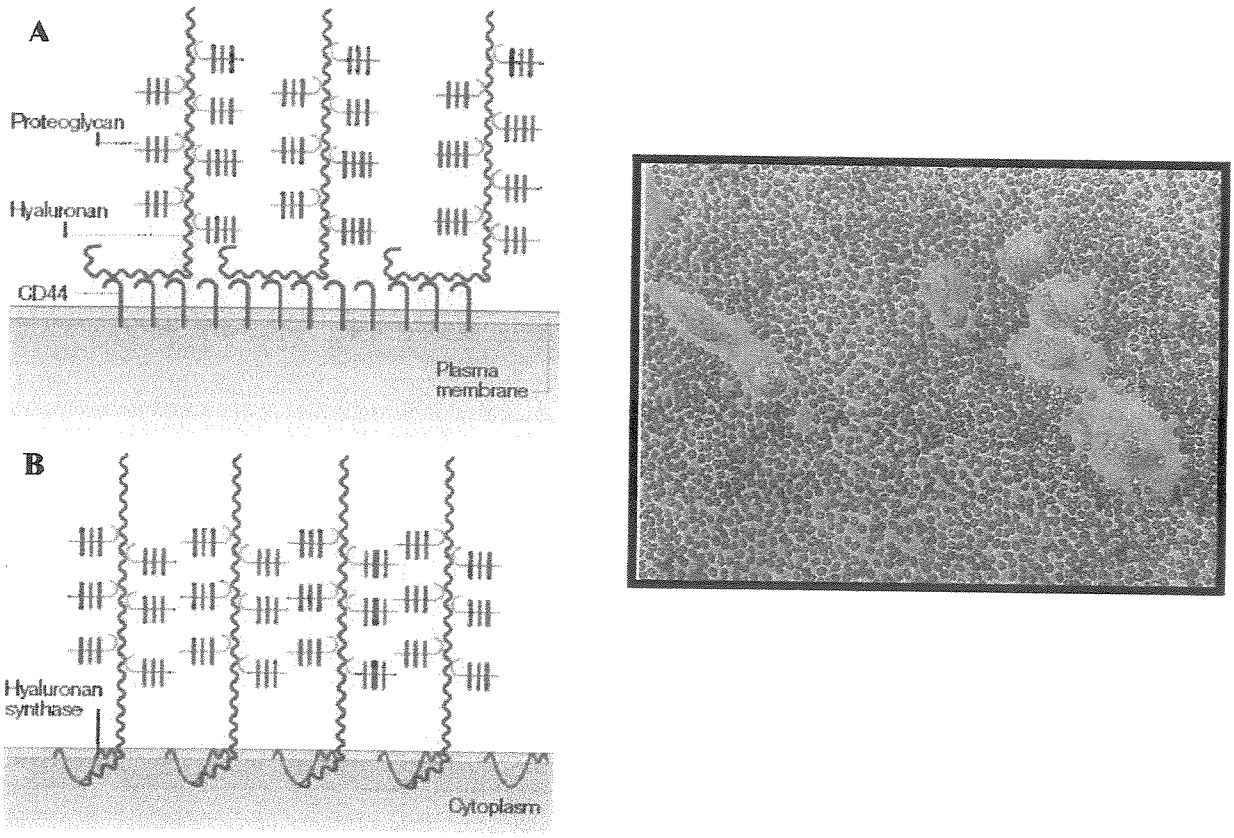

Figura 4. O AH pode estar associado à membrana plasmática das células através do receptor CD44 (A) ou através da HAS que, ao sintetizar o AH, não libera a molécula, ficando esta presa à enzima (B) (Reproduzido de Toole, 2004). À direita, são mostradas células PC3, onde se nota a presença de um halo ao redor das células, que não permite que as hemácias aproximem-se da membrana celular.

Alguns autores têm descrito que cadeias de AH com massas moleculares maiores que 10^6 Da estão envolvidas na manutenção da estrutura e na viscosidade do tecido (Laurent et al., 1996), na adesão célula-matriz extracelular (Zimmermam et al., 2002) e na redução da inibição por contato, promovendo migração celular e metástase (Ichikawa et al., 1999, Itano et al., 1999b, Kosaki et al., 1999, Liu et al., 2001, Itano et al., 2002). Por outro lado, cadeias de AH com massas moleculares menores que 10^6 Da estão envolvidas em processos de angiogênese, proliferação celular, migração e inflamação (Jacobson et al., 2000).

Um fato interessante é que a própria célula pode manipular as propriedades do AH produzido a seu favor, através do controle da expressão das diferentes enzimas que sintetizam o AH. Este controle depende do estágio de desenvolvimento, do tipo de tecido e dos estímulos externos que são enviados às células (Spicer & McDonald, 1998, Jacobson et al., 2000, Rosa et al., 1988, Koprunner et al., 2000, Sayo et al., 2002). As hialuronidases também apresentam papel ativo na formação de cadeias de AH de diferentes tamanhos, podendo gerar fragmentos que desenvolverão um estímulo ao organismo para uma resposta anti-inflamatória, por exemplo. A digestão de AH com Hyal-2 pode produzir fragmentos de 20 kDa, que foram capazes de estimular a síntese de citocinas inflamatórias pelas células (Noble, 2002). Muitos outros produtos da degradação enzimática realizada pelas hialuronidases podem gerar respostas celulares como indução de expressão de HSP (*heat-shock protein*), prevenir apoptose e produzir efeitos contrários como inflamação e tumorigênese (Stern, 2003).

A próstata

O aparelho reprodutor masculino possui um conjunto de glândulas acessórias, que inclui a próstata, a vesícula seminal e a glândula coaguladora, que em alguns casos é também denominada de próstata anterior. Todas estas glândulas localizam-se próximas da bexiga e, no homem, estão circundando a uretra. Nos roedores, há uma diferenciação da próstata, que se apresenta em 3 pares de lobos: ventral, dorsal e lateral. Na Fig. 5 é possível verificar a distribuição da próstata no aparelho reprodutor masculino no homem e nos roedores.

A próstata tem como principal função produzir o líquido prostático, que corresponde à porção significativa do sêmen. O desenvolvimento, bem como as funções da próstata são controladas pelos hormônios androgênicos, em especial a testosterona e seu mais potente metabólito, a diidrotestosterona (DHT). Compõem o tecido prostático células epiteliais, células musculares lisas, fibroblastos, mastócitos, células endoteliais, pericitos, terminações nervosas e gânglios sensitivos. A matriz extracelular está representada por componentes da

membrana basal, colágenos, proteoglicanos, ácido hialurônico e elastina (Carvalho & Line, 1996; Carvalho et al., 1997).

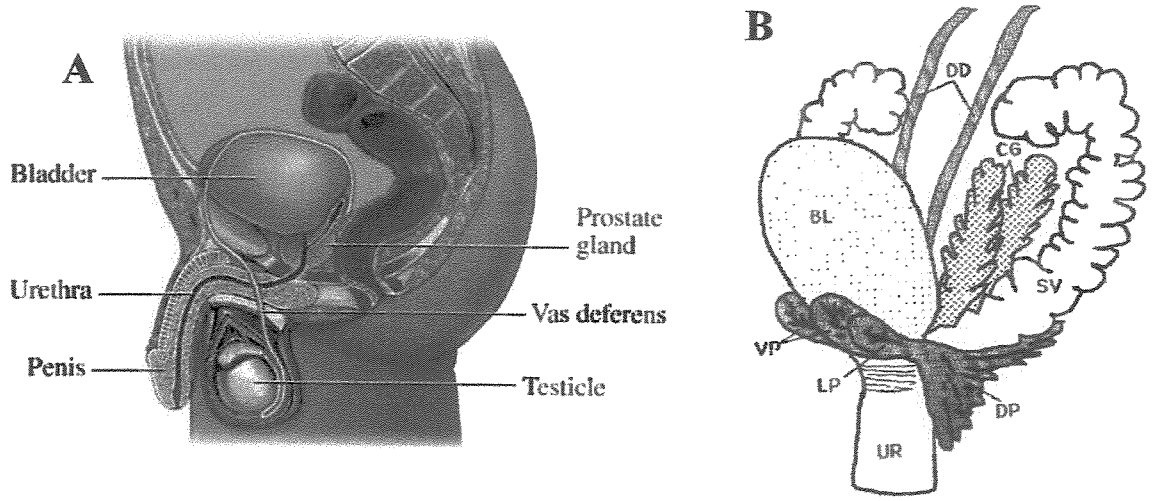

Figura 5. Posição anatômica da próstata e sua relação com as glândulas acessórias vizinhas. **A.** Próstata humana (reproduzido de www.medical-malpractice-lawyers-attorneys.com); **B.** Próstata de roedores, que se divide em lobos ventrais (VP), dorsais (DP) e laterais (LP). Estão também representados a uretra (UR), a vesícula seminal (SV), a glândula de coagulação (CG), os ductos deferentes (DD) e a bexiga (BL) (reproduzido de Sugimura et al., 1986).

A estimulação por andrógenos é absolutamente necessária para o desenvolvimento da próstata, assim como para as demais estruturas sexuais masculinas (Cunha et al., 1987). A produção de andrógenos pelos testículos do feto começa antes da morfogênese prostática (Pointis et al., 1980) e o desenvolvimento da próstata não é determinado pelo sexo genético, mas sim pela exposição a estes andrógenos. Foi demonstrado que o seio urogenital (UGS) da fêmea ou do macho pode formar tecido prostático funcional, caso eles sejam estimulados por andrógenos no período adequado (Takeda et al., 1986).

O brotamento prostático, bem como a morfogênese ductal, a canalização e a citodiferenciação epitelial são iniciados pela ação androgênica pré-natal (Timms et al. 1994). Embora a testosterona seja o primeiro andrógeno produzido pelos testículos fetais, a DHT é a responsável pela morfogênese prostática (Taplin & Ho, 2001). A DHT é produzida no UGS por redução da testosterona pela 5α-redutase.

No rato, a maior parte da ramificação dos ductos ocorre logo após o nascimento, quando os níveis de andrógenos são extremamente baixos (Donjacour et al., 1988). A

diferenciação do epitélio prostático ocorre paralelamente à maturação do estroma. Andrógenos atuam sobre seus receptores (AR) no mesênquima urogenital (UGM) para induzir a proliferação das células epiteliais, ramificação ductal e citodiferenciação nos subtipos celulares glandulares basal e luminal (Cunha et al., 1987; 1992). Por sua vez, o epitélio prostático em desenvolvimento direciona os padrões de diferenciação do músculo liso prostático (Hayward et al., 1998). O desenvolvimento do epitélio e do músculo liso é interdependente, ou seja, um não se desenvolve sem a presença do outro tecido (Hayward e Cunha, 2000).

Recentemente foi demonstrado que, durante a organogênese, uma das funções dos andrógenos é reduzir a camada de células musculares lisas que envolve a uretra. Quando esta camada é espessa, dada a ausência de andrógenos, como acontece nas fêmeas, o brotamento inicial a partir da uretra não consegue atingir o mesênquima do seio urogenital e o desenvolvimento prostático não ocorre (Thomson et al., 2002).

No período pós-natal, o desenvolvimento prostático é também dependente de andrógenos já que a castração de ratos neonatos inibe o crescimento e desenvolvimento da próstata durante a puberdade, um efeito que pode ser revertido pela administração de testosterona (Cunha et al., 1987; Corbier et al., 1995). A administração de testosterona acelera o crescimento da próstata, sendo possível atingir precocemente o crescimento máximo (Berry & Isaacs, 1984). Na puberdade tem-se o início do crescimento prostático, que é caracterizado pelo aumento de peso da próstata e por um pequeno incremento no número das ramificações (Sugimura et al., 1986). Estes dados sugerem que a próstata em desenvolvimento é sensível às baixas concentrações de andrógenos para a ramificação ductal e que a sua resposta aos níveis de andrógenos altos na puberdade (aumento de peso da glândula) é diferente da resposta inicial de ramificação ductal (Hayward & Cunha, 2000).

No crescimento prostático pós-natal, o AH apresenta-se como uma molécula de vital importância para o processo de ramificação dos ductos. A presença do receptor CD44 é imprescindível para que o AH exerça a função de regulador da ramificação ductal da próstata de ratos (Gakunga et al., 1997).

Em roedores adultos, no que diz respeito ao aspecto histológico, a próstata ventral

apresenta-se composta por um conjunto de ductos formados por células epiteliais que se originam da uretra e esses ductos são envolvidos por um estroma. Foram identificados oito ductos principais, que se ramificam distalmente. Os ductos podem ser divididos em três regiões morfológica e funcionalmente distintas, denominadas de proximal, intermediária e distal, de acordo com a sua posição em relação à uretra (Lee, 1990; Shabsigh et al., 1999). Na região distal são encontradas células epiteliais colunares altas com atividade proliferativa circundadas por células musculares lisas que formam uma camada esparsa e descontínua, associadas a um grande número de fibroblastos (Nemeth & Lee, 1996). Na região intermediária as células epiteliais também são colunares altas, apresentando características de células secretoras, porém sem atividade proliferativa, sendo que a camada de células musculares lisas é fina e contínua. Na região proximal as células epiteliais são cúbicas e baixas, sendo freqüentes células apoptóticas. Nesta região, as células musculares lisas formam uma camada espessa ao redor dos ductos. Tanto na região intermediária como na proximal, a matriz extracelular está presente no espaço entre os ductos e, ocasionalmente, insere-se entre camadas de células musculares lisas. Como em qualquer glândula, a atividade das células epiteliais é fortemente influenciada pelos componentes estromais. Assim, as diferenças fenotípicas das células epiteliais encontradas ao longo dos ductos prostáticos parecem estar relacionadas à distribuição diferenciada dos fibroblastos e das células musculares lisas (Prins, 1992; Lee et al., 1990; Nemeth & Lee, 1996).

Em estudo recente, Kurita e colaboradores (2001) demonstraram a importância da interação epitélio-estroma no processo de manutenção do órgão, sendo que, na presença de andrógenos, as células estromais enviam sinais de sobrevivência (ou anti-apoptóticos) às células epiteliais. Na ausência dos hormônios androgênicos, as células estromais deixam de enviar os sinais de sobrevivência para as células epiteliais ou produzem sinais apoptóticos, que também são enviados às células epiteliais, potencializando o efeito de morte celular causado pela ausência dos andrógenos (Fig. 6).

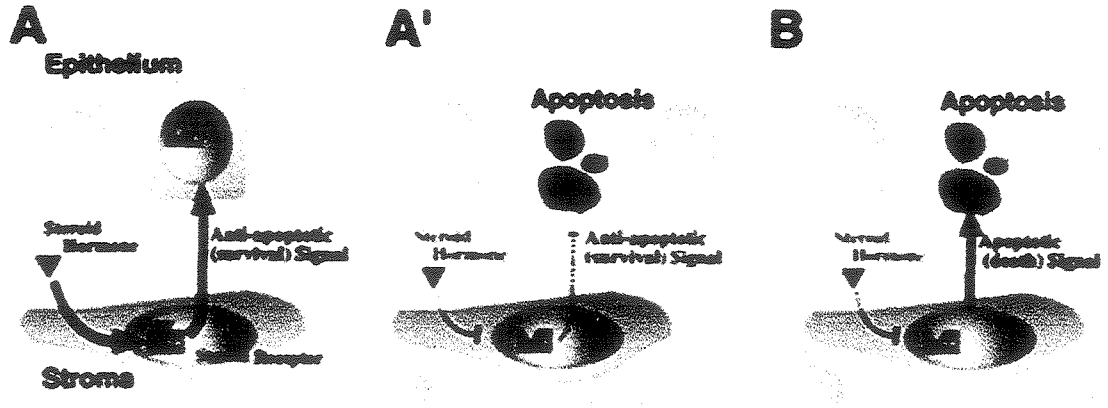

Figura 6. Mecanismo parácrino de regulação de células epiteliais prostáticas. **A.** Condições normais, na presença de andrógeno, as células estromais enviam o sinal de sobrevivência. Na ausência do andrógeno, deixam de ser enviados sinais de sobrevivência (**A'**) e passam a ser enviados sinais de morte ou apoptose (**B**). Reproduzido de Kurita et al., 2001.

As células musculares lisas (CML) representam 22% da área total da próstata humana (Shapiro et al., 1992), predominando ao redor dos ductos, onde se encontram em íntimo contato com a membrana basal das células epiteliais. Já na próstata ventral de ratos, as CML ocupam cerca de 5% do volume total da glândula e cerca de 14% do estroma (Antonioli et al., 2004). As CML apresentam papel preponderante nos mecanismos de estimulação parácrina sobre o epitélio (Farnsworth, 1999) e provavelmente também sobre as demais células estromais.

Ainda no que diz respeito à regulação e manutenção da atividade funcional da próstata, destaca-se o papel desempenhado pelas interações epitélio-estroma (Lee, 1996). Dentre os elementos destas interações, destaca-se a membrana basal. Esta estrutura é extremamente importante no controle das atividades celulares e, principalmente, na manutenção da fisiologia das células epiteliais (Hayward et al. 1998). Composta principalmente de colágeno tipo IV e laminina, a membrana basal é essencial para a manutenção do fenótipo diferenciado e secretor das células epiteliais glandulares (Labat-Robert et al., 1990). Os principais componentes das membranas basais foram detectados na próstata humana normal (Knox et al., 1994) e nas membranas basais dos carcinomas com diferentes graus de diferenciação tumoral, com exceção do colágeno do tipo VII, que está ausente dos ductos neoplásicos.

Um dos modelos de estudo para a próstata que vêm sendo utilizado com freqüência é a privação de andrógenos, na maioria dos casos obtida por castração cirúrgica. Após a retirada dos testículos, cerca de 95% da testosterona circulante é eliminada. Como resultado ocorre involução da próstata e das outras glândulas acessórias do aparelho reprodutor masculino.

Carvalho & Line (1996) descreveram as modificações associadas à membrana basal das células epiteliais e das células musculares lisas prostáticas ocorridas após a castração. Os autores demonstraram que eventos apoptóticos seguem-se à perda de adesão da célula à membrana basal e que existe um retardo na absorção das membranas basais residuais, as quais se tornam extremamente pregueadas e laminadas e apresentam moléculas intactas de laminina, mesmo 21 dias após a castração.

Ilio e colaboradores (2000) observaram que a laminina está presente uniformemente na membrana basal ao longo dos ductos prostáticos, enquanto o colágeno tipo IV é encontrado na membrana basal da região distal e intermediária, embora esteja praticamente ausente na região proximal. Demonstraram também que o processo de involução prostática após a castração inicia-se com a perda ou redução do colágeno tipo IV, nas diferentes regiões dos ductos, durante os primeiros dias após a castração, enquanto a laminina permanece intacta, sugerindo que pode ocorrer uma associação direta entre aumento de apoptose e diminuição de colágeno tipo IV.

As fibras de colágeno tipo I e tipo III que compõem a matriz extracelular do estroma sofrem um amplo rearranjo na próstata em regressão. Este rearranjo é caracterizado por um aspecto pregueado das fibras ao redor dos ductos e está intimamente associado às funções assumidas pelas células musculares lisas após a castração (Vilamaior et al., 2000).

As microfibrilas de colágeno tipo VI e fibras do sistema elástico também são encontradas no estroma prostático e apresentam modificações durante a involução do órgão. Estes componentes parecem estar envolvidos no controle de alguns aspectos do comportamento celular e desempenham um papel estrutural, mantendo a integridade do órgão (Carvalho e Line, 1996; Carvalho et al., 1997).

Também no estroma são encontrados proteoglicanos e ácido hialurônico, além de outros componentes de matriz extracelular, que têm seu conteúdo alterado em função da

presença ou ausência de hormônios androgênicos. Kofoed e colaboradores (1990) verificaram que a castração induz um aumento considerável no conteúdo de proteoglicanos na próstata ventral de ratos, identificado pelo aumento na concentração de condroitim sulfato, acompanhado também de um aumento de ácido hialurônico. Variações no conteúdo de condroitim sulfato são aparentemente devidas a uma maior expressão de um proteoglicano de condroitim/dermatam sulfato durante a hiperplasia prostática e durante a atrofia glandular (Walden et al. 1998).

Considerações gerais

A próstata é um órgão que tem seu desenvolvimento e sua atividade funcional controlada pela ação de hormônios androgênicos, em especial a testosterona e seu principal metabólito, a diidrotestosterona. Variações com respeito à quantidade destes hormônios no organismo causam alterações estruturais e funcionais na próstata. A castração cirúrgica, com a retirada dos testículos, faz com que ocorra uma queda de cerca de 95% da testosterona circulante, representada pela síntese deste hormônio pelos testículos. Os 5% remanescentes são produzidos pela glândula adrenal, que, por sua vez, não são capazes de manter o estado fisiológico da próstata.

A retirada da testosterona circulante causa uma regressão do órgão, caracterizada pela perda de massa e volume e por alterações morfológicas, como aumento de estroma, abaixamento do epitélio e perda de adesão destas células à membrana basal. Além disso, vários componentes de matriz extracelular têm seus níveis de expressão alterados. Por outro lado, a administração de testosterona reverte o quadro de regressão tecidual, com a recomposição do órgão, tanto em massa e volume quanto ao retorno de seu estado funcional, caracterizado pelo aumento da altura do epitélio e pela síntese de proteínas que compõem o líquido prostático. Desta forma, o modelo experimental de castração cirúrgica apresenta-se como um sistema adequado para o estudo de remodelação tecidual, uma vez que após a castração, a regressão tecidual ocorre em um período relativamente curto, bem como a reestruturação do órgão após a administração de testosterona.

Dentre os componentes de matriz extracelular, o AH apresenta-se como uma molécula importante para os tecidos na estruturação da matriz extracelular (seja por reter água no tecido, seja por se agregar com proteoglicanos) e no controle do comportamento celular (modulando e/ou permitindo a migração celular e outros processos), por ligarem-se a receptores específicos, além de criar um microambiente pericelular onde atua como proteção mecânica, na exclusão de outras macromoléculas e de material particulado e na agregação de fatores de crescimento.

Em processos de remodelação tecidual, a importância do AH está associada à sua participação no processo de regeneração tecidual, amplamente descrito em processos de cicatrização. A participação do AH especificamente neste processo é de grande importância, pois, dentre outras funções, auxilia no processo de migração celular e agregação de fatores de crescimento e outros componentes necessários ao processo de reconstituição do tecido lesionado.

Assim, o estudo do AH no modelo de castração cirúrgica pode contribuir para a compreensão da amplitude das alterações causadas pela retirada de testosterona, a partir da reprogramação das células estromais frente à privação androgênica, com conseqüente reorganização da matriz extracelular como um todo.

Objetivos

OBJETIVOS

Visando ampliar a compreensão dos mecanismos envolvidos com a remodelação tecidual prostática seguida à castração, assim como o envolvimento dos diferentes tipos celulares neste processo, e considerada a importância do AH em diversos processos celulares, a presente tese tem como objetivos:

1. Definir a distribuição tecidual do AH, quantificar as variações de conteúdo promovidas pela castração e verificar os níveis de expressão de RNAm das enzimas que sintetizam e degradam o AH,
2. Descrever a distribuição do CD44,
3. Determinar os níveis de expressão do RNAm da HAS2 e da Hyal1 e
4. Definir o papel das células musculares lisas na produção de AH, *in vitro*, sob o estímulo hormonal de testosterona e insulina.

De acordo com os resultados obtidos, este trabalho pretende fornecer dados para o entendimento do processo de remodelação tecidual, que tem como modelo a involução prostática frente à retirada da testosterona circulante.

Artigos

Artigo 1

Effects of castration on hyaluronan synthesis and degradation in the rat ventral prostate

A ser submetido ao Journal of Cell Science

Effects of castration on hyaluronan synthesis and degradation in the rat ventral prostate

Heloisa H. M. Della Colleta[1], Sara T. O. Saad[2], Hernandes F Carvalho[1]
[1]Department of Cell Biology, Institute of Biology and [2]Department of Clinical Medicine,
Faculty of Medicine, State University of Campinas – UNICAMP
Campinas SP, Brazil

Corresponding author: Hernandes F Carvalho
Department of Cell Biology – UNICAMP
CP6109
13083-063 Campinas SP, Brazil
Tel. 55 19 3788 6118
Fax 55 19 3788 6111
E-mail hern@unicamp.br

Key-words: hyaluronan, prostate, castration, HAS, Hyal

Running header: Hyaluronan metabolism in the prostate

Summary

Hyaluronan (HA) has been implicated in prostate cancer progression and appears as a strong diagnosing molecule. Furthermore, it is involved in important phenomena besides tumor growth, such as tissue remodeling and healing, which include aspects of cell proliferation and migration. This work was undertaken to define some aspects of HA metabolism in the rat ventral prostate in association with the extensive tissue remodeling occurring in response to androgen deprivation. We have examined hyaluronan content, distribution, size variation, hyaluronan synthase 2 (HAS2) and hyaluronidase 1 (Hyal1) mRNA expression, acidic hyaluronidase activity and CD44 distribution in the rat ventral prostate and their variations attained by castration. The results demonstrated an overall reduction in HA, though associated with increasing concentration. The chain size showed an increase in long chains 7 days after castration and a posterior reduction, associated with increased content in short HA size chains. HA was located in both epithelium and stroma in the prostate of both non-castrated and castrated animals. HAS2 and Hyal1 mRNA were demonstrated to be found in both epithelial and stromal cells, indicating the involvement of both compartments in HA synthetic and degradation activities. Smooth muscle cells and endothelial cells are among the stromal cells which showed very little expression of both mRNAs. Real time PCR showed that, while HAS2 mRNA presents no defined variation tendency with androgen deprivation, Hyal1 increased progressively after castration. Acid hyaluronidase activity was demonstrated to decrease after castration. CD44 was found in the epithelial cells and in some stromal cells in both hormonal situations. It seems that HA dynamics in the prostate results from the balance between synthesis and degradation activities expressed by both epithelium and stroma. Furthermore, it is concluded that there is a predominant non-lysosomal hyaluronidase activity after castration, which results in a decrease of the total amount of HA and in the accumulation of short sized molecules.

Introduction

Hyaluronan (HA) is a major component of the extracellular matrix and predominates whenever rapid cell proliferation, migration, and tissue repair occur (Laurent and Fraser, 1992, Fraser et al., 1997). In addition, HA acts as a hydrated, space-filling material and as a lubricant for tissue movement. Moreover, it stabilizes the extracellular matrix in many tissues by binding to the so called hyaladherins.

Hyaluronan has been implicated in some aspects of prostate cancer progression and diagnosis (Lokeshwar et al., 1999). It was demonstrated that strong stromal HA expression is related to PSA recurrence, perineural infiltration and seminal vesicle invasion (Aaltomaa et al., 2002). It is also worth mentioning that hyaluronan production is involved with cancer progression, since the HAS2 gene was demonstrated to be located in a minimally overexpressed region (8q24) identified in prostate cancer, together with c-myc and other 5 genes (Tsuchiya et al., 2002). Reinforcing the involvement of hyaluronan in cancer progression is the demonstration that inhibition of hyaluronan synthesis impaired vascularization and subcutaneous growth of implanted cancer cells (Simpson et al., 2002a).

Given the involvement of hyaluronan in prostate cancer, we decided to investigated some aspects of hyaluronan biology in the rat ventral prostate. Kofoed et al. (1990) have shown that uronic acid concentration increases in the rat prostate lobes after castration and that this involves variations in different glycosaminoglycans, including HA. Terry and Clark (1996) have then demonstrated that the absolute amount of HA in the ventral prostate decreases 74% after seven days of androgen deprivation and concluded that the glycosaminoglycans are regulated by androgens.

Beside this variation in HA content, the stroma of the rat ventral prostate exhibits other changes related to the remodeling process. We have previously characterized the presence and behavior of different extracellular matrix components. The epithelial basement membrane was shown to be pleated and folded by the remaining epithelial cells (Carvalho and Line, 1996), and variations in elastin-associated microfibrils (Carvalho et al., 1997a), type VI collagen (Carvalho et al., 1997b) and collagen fibers (Vilamaior et al., 2000) were also demonstrated.

This work has been carried out aiming at confirming previous results on HA content, using a different quantitation protocol, to localize HA in the different tissue compartments and define some aspects of its biosynthesis and degradation, examining the expression of HAS2 and Hyal1, a hyaluronan synthase and a hyaluronidase, respectively, at the mRNA level, in association with the determination of hyaluronidase activity, and localization of CD44.

As a matter of fact, three enzymes are involved with HA biosynthesis, i.e. HAS1, HAS2 and HAS3 and three hyaluronidases are involved with HA degradation. Our choice in studying HAS2 is because it has a direct correlation with chromosomal changes found in prostate cancer (Tsuchyia et al., 2002) and Hyal1 is the plasma hyaluronidase with prognostic value for prostate cancer (Lokeshwar and Rubinowicz, 1999).

The series of results demonstrated that castration promotes an overall reduction in HA content per prostate with greater contribution of short sized chains and that this pattern results from a sustained hyaluronan synthase expression and increased non-lysosomal hyaluronidase activity.

Materials and Methods

Materials

All reagents were molecular biology grade and were purchased from either Sigma Chemical Co. (Saint Louis MO, USA) or Merck (Darmstadt, Germany), unless otherwise mentioned.

Animals

Three-month-old Wistar rats were purchased from CEMIB-UNICAMP. The rats were subjected to orchiectomy through scrotal incision under chloral hydrate (0.3 mg/kg) anesthesia. Ventral prostates were removed 7, 14 and 21 days after castration and sham operated, age-matched rats were employed as controls, performing 4 experimental groups.

HA extracts

For each group, ten ventral prostates were removed and placed in acetone overnight for delipidation. The specimens were dried and pulverized. HA extraction was made using papain digestion. For 100 mg dried tissue, 2 mL digestion buffer (100 mM NaAc, 5 mM cystein, 10 mM EDTA, pH 5.5), containing 1.5 mg papain/mL were used. The digestion was carried out at 60°C for 24 h, centrifuged (1000 x g, 20 minutes) and the supernatant was collected. Ice cold ethyl alcohol was added to the supernantants (2 mL alcohol:1 mL sample) and kept overnight at – 20°C. Samples were centrifuged (1000 x g) for 20 minutes and the pellets were ressuspended in water and heated to 60°C for 10 minutes. The samples were stored at 4°C.

HA probe preparation

The procedure used for isolation of HA-binding protein was described previously (Tengblad, 1979). Briefly, bovine femoral cartilage was extracted with 4 M guanidine hydrochloride (Gn-HCl) containing proteinase inhibitors. The Gn-HCl extract was then dialysed against 0.4M Gn-HCl to attain aggregate formation and then subjected to ultracentrifugation in cesium chloride density gradient. The A1 fraction of the ultracentrifugation was dialysed against 0.1 M Tris, 0.03 M NaAc, pH 7.4 and digested with trypsin (0.25 mg/mL) overnight at 37°C. The HA-binding proteins and HA was separated by cromatography on a Sepharose CL6B column (Amersham, Buckinghamshire, England) and then dialysed against Gn-HCl. The HA-binding protein was finally purified by Superose 6 column cromatography using an AKTA purifier system (Amersham).

The purified HA-binding protein (mostly aggrecan-G1 and link protein) was biotinylated using EZ-Link™ Sulfo-NHS-LC-Biotin (Pierce Biotechnology Inc, Rockford IL, USA). In brief, one milligram of protein was mixed with 500 µl sodium bicarbonate buffer (50 mM, pH 8.3) and 40 µL of biotin (1mg/mL) for 2 hours in ice. Unbound biotin was separated after centrifugation with microconcentrator ultrafree-MC (Millipore, Billerica MA, USA.) and stored in the dark at – 20°C.

Alternatively, the HA probe was labeled with fluorescein isothiocyanate (FITC). The probe was dialysed against carbonate-bicarbonate buffer pH 9.2 and then mixed with 375 μM FITC for 4 h at room temperature. Unbound FITC was removed through cromatography on Superose 6 with PBS (5 mM phosphate, 0.15 M NaCl pH 7.4). The eluate was monitored by the absorbance at 495 nm and the fractions containing the FITC-conjugated proteins were concentrated and stored in the dark at – 20°C.

Measurement of HA content

The concentration of HA in ventral prostates extracts was determined in a competitive binding assay (Lokeshwar et al., 1997). Briefly, 96-well microtiter plates (Corning 1550) were coated with HA (Sigma Chemical Co.) at 25 μg/mL in 200 mM carbonate buffer (pH 9.6) for 4 hours at 37°C. Excess HA was removed with four washes of PBS/0.05% Tween 20. Serial dilutions of HA extract were combined with biotinylated hyaluronic acid-binding protein and incubated in the HA-precoated wells at room temperature overnight. The plate was washed 4X with PBS/Tween 20, developed using avidin-HRP with OPD (o-phenylenediamine) as a substrate, and read at 490 nm. HA concentration was interpolated from a standard curve generated by plotting HA concentration against absorbance values. The results present the mean of four different experiments made in triplicate for each group.

Determination of HA chain size variation

HA extracts were subjected to gel cromatography on a gel Sepharose CL 6B (Amersham) column (120 x 0.6 cm) in sodium acetate 0.05 M, pH 5.8 buffer. One mL fractions were collected and assayed for the presence of HA (see HA content measurement above). HA chains were classified in three size groups. The void and total volume of the column was 13 mL and 36 mL, as determined by Blue Dextran 2000 and copper sulphate, respectively.

HA in situ detection

The localization of HA in prostate tissue sections was done using the FITC-labeled probe applied to 7 μm frozen sections. Peroxidase treatment (3% H_2O_2 in water) for 15 min was

done to eliminate auto-fluorescence and non-specific binding sites were blocked with 3% bovine serum albumin (BSA) in TBS-T (0.05 M Tris, 0.15 M NaCl, pH 7.4 with 0.1% Triton X-100). The sections were incubated with the probe diluted in 1% BSA for 2 hours at room temperature. The slides were washed with TBS-T, mounted using Vectashield (Vector Laboratories, Burlingane CA, USA) and photographed in a Zeiss Axioskop fluorescence microscope. The specificity of the staining was controlled by digesting some sections with *Streptomyces hyaluronidase* prior to incubation with the probe. In this latter case, nuclei were stained with DAPI.

HAS2 and Hyal1 in situ hybridization

For in situ hybridization, specimens were collected and frozen immediately at liquid nitrogen and then stored at - 70°C. All the solutions were made with DEPC (diethyl pyrocarbonate) treated water and autoclaved. The sequences of rat HAS2 and Hyal1 were found in PubMed bank and the probes were designed using an internet progam (www.genome.wi.mit.edu/cgi_bin/primer/primer3_www). The biotinylated probes HAS2 5' - biotin - GATTGTAAACCACACGGACACTGGAATAAG - 3' and Hyal1 5' - biotin TTCAGGCACCAGTGAGTGTCTGCATTCCAA - 3' were synthesized by Invitrogen Life Technologies (Carlsbad CA, USA).

Frozen sections were air dried for 30 minutes, fixed using ice cold 4% paraformaldehyde in PBS for 5 minutes, air dried for 30 minutes and washed with TEA buffer (1.34% triethanolamine) for 2 minutes. The sections were incubated with 0.25% acetic anhydride in TEA buffer, under magnetic stirring. After 10 minutes the slides were washed with SSC 2x and dehydrated with ethanol 70% (2 minutes), 95% (2 minutes), 100% (2 minutes), chloroform (5 minutes), ethanol 100% (2 minutes) and 95% (2 minutes). The sections were washed with pronase buffer (50 mM Tris-HCl pH 7.5 (Merck) and 5 mM EDTA pH 8, at 37°C and incubated with 125 μg/mL pronase for 10 min at 37°C. The sections were washed with 0.1M sodium phosphate twice and fixed with 4% paraformaldehyde at room temperature for 10 minutes. After fixation, the slides were washed twice with 0.1 M sodium phosphate, once with water and partially dehydrated with two changes of 70% ethanol.

The hybridization mix was composed by 31.25% formamide, 12.5% Dextran, 375 mM NaCl, 10 mM Tris-HCl pH 8, 1.12 mM EDTA, Denhardt's solution (1.25X final concenctration) and 0.01M dl-Dithiothreitol. The probe mix was composed by 2 pmol of probe (2/4 of volume), tRNA (¼ of volume) and TED (¼ of volume). The final solution was composed by 4 parts of hybridization mix and 1 part of probe mix. The mixture was placed over the sections and the slides were covered with plastic film and incubated at 37°C overnight in a humidified chamber.

After hybridization, the sections were washed twice with SSC 2x buffer for 30 minutes each wash. The sections were incubated with 3% H_2O_2 in methanol for 30 minutes at room temperature and washed 3 times with TBS (Tris buffer saline) 5 minutes each one. The protein-protein block was done with 1.5% fetal calf serum (FCS, Nutricell, Campinas SP, Brazil), 0.1% gelatin, 0.2% bovine serum albumin in TBS for 1 hour at room temperature. The detection of the hybridization product was done using ABC kit (Vector Laboratories). The slides were counterstained with Hematoxilin, air dried, cleared in xylene and mounted in Entellan.

RNA extraction and reverse transcription

Total RNA extraction was performed using Trizol reagent (Invitrogen Life Technologies). Samples (50 mg) were homogeneized in 1 mL of Trizol using a Polytron homogenizer (Kinematica, Lucerne, Switzerland) and the subsequent procedures were carried out according to manufacturer. The RNA integrity was analyzed by electrophoresis in 1.2% denaturing agarose gel and RNA concentration was quantified by spectrophotometry using a Ultraspec 2100 pro equipment (Amersham).

Five-microgram RNA samples were incubated with 1 U DNaseI (Promega, Madison WI, USA) for 15 minutes at room temperature, and EDTA was added to a final concentration of 2 mM to stop the reaction. The enzyme was subsequently inactivated for 10 minutes at 65°C. The DNaseI-treated RNA samples were reverse transcribed with 200 U SuperScript III (Invitrogen Life Technologies) for 50 minutes at 42°C. Two units of RNase H (Promega) were subsequently added, and the samples were incubated at 37°C for 20 minutes. The cDNA was quantified by spectrophotometry as above.

Real-time polymerase chain reaction

Real-time polymerase chain reaction (PCR) using SYBR Green dye is based on the direct detection of the PCR product, as monitored by measuring the increase in fluorescence caused by the binding of SYBR Green dye to double-stranded DNA. An increased amount of PCR product will result in an increase in SYBR Green dye fluorescence, which is monitored during the course of reaction. The resulting real-time analysis enables a more accurate quantification of nucleic acids (Higuchi et al., 1993, Bustin 2000, Deprez et al., 2002).Quantification of *HAS2* and *Hyal1* gene expression by real-time PCR was performed using a 5700 Applied Biosystems (Foster City CA, USA) system. Quantification of *β-actin* expression was used as an internal control for the amount and quality of cDNA.

To quantify gene expression, a mathematical model, using calibration data ($2^{(-\Delta\Delta Ct)}$) was used. For *HAS2* and *Hyal1* expression in the rat ventral prostate of castrated and non-castrated rats, expression measured for non-castrated rats was used for data calibration. For this mathematical model, determination of the crossing threshold (Ct) was necessary for each transcript. Ct was defined as the point at which the fluorescence rises appreciably above the background fluorescence. The dissociation protocol was performed at the end of each run to check for non-specific amplification. Two replicas were run on the plate for each sample, and each sample was run twice, independently.

Synthetic oligonucleotide primers were designed using Primer Express software (Applied Biosystems) and synthesized by Invitrogen. The sequences of the primers were β-actin forward: 5′-CTGGCCTCACTGTCCACCTT-3′; β-actin reverse:5′-GGGCCGGACTCATCGTACT-3′; HAS2 forward: 5′-TGGCTGGTGTCCAGTGCATAAG-3′; HAS2 reverse: 5′-TGGTTACCCATGAATTCCTGATT-3′; Hyal1 forward: 5′-TTCTCCATTGAGCTAACACATGATG-3′; Hyal1 reverse: 5′ - TCACACCACTTGCCTCTCCAT-3′.

All samples were assayed in duplicate in a semi-kirted PCR 96-well reaction plate (Sorenson, BioScience Inc., Salt Lake City UT, USA) with eight-strip PCR tube caps (SSI) and performed in a 25 μL volume containing 20 ng cDNA per μL, 12.5 μL SYBR Green Master Mix PCR (Apllied Biosystems) 900 μM each primer. To confirm accuracy and

reproducibility of real-time PCR, intra-assay precision was calculated according to the equation: $E^{(-1/slope)}$, where the PCR efficiency was calculated (Pfaffi, 2001, Meijerink et al., 2001). The investigated transcripts showed high real-time efficience rates (Pearson correlation coefficient $r > 0.95$).

Hyaluronidase zymography

Hyaluronidase was extract from tissues immediately after dissection, using protocol established by (2000). The prostates were subjected to enzymatic digestion in 1 mL trypsin-EDTA solution supplemented with 1 mg/mL collagenase D and 1 mg/mL BSA. The tissues were disrupted with a Polytron and incubated for 2 h at 37 °C. The material was centrifuged at 200 x g for 10 minutes, and the supernatant was collected and dialyzed against 0.1 M sodium formate, 0.15 M NaCl pH 3.7. Samples to be examined for the presence of HAase activity were electrophoresed on 7.5 % SDS-polyacrylamide gels. An aqueous stock solution of 1 mg/mL HA (Sigma) was prepared and kept overnight at 4°C without stirring. This solution was added to the gelling mixture in an amount that would make the final concentration of 170 μg/mL of HA in the separating gel. Forty micrograms of total protein (measured by Bradford kit) were submitted to gel zymography. The samples was diluted in Laemmli's sample buffer under non-reducing conditions, without heating and applied to the slot gel. After electrophoresis, the gel was rinsed with 3.0% Triton X-100 for 1 hour at room temperature. Then, the gel was incubated with 0.1 M sodium formate, 0.15 M NaCl pH 3.7 for 16 h at 37°C. After staining the gel with alcian blue (0.5% alcian blue in 20% ethanol and 10% acetic acid) for 1 hour following incubation, unstained bands could be seen after washes with 20% ethanol and 10% acetic acid.

CD44 immunohistochemistry

CD44 was localized by using a rabbit polyclonal anti-CD44 (Santa Cruz Biotech, Santa Cruz CA, USA). Endogenous peroxidase was blocked by incubating the sections with 3% H_2O_2 (in water) for 20 minutes. Non-specific protein binding was blocked with 3% BSA in TBS-T. The sections were incubated with the antibody diluted in 1% BSA overnight at 4°C. The slides were washed with TBS-T and incubated with HRP-labeled anti rabbit Ig

antibody for 2 hours at room temperature. The slides were washed with TBS-T and developed with 0.05% 3, 3′-diaminobenzidine tetrahydrochloride and 0.03% hydrogen peroxide in phosphate buffer (0.05 M, pH 7.4) at room temperature. The slides were counterstained with methyl green for 15 min, washed, air dried and mounted in Entellan.

Results

Effects of castration in prostate weight and HA levels

Castration resulted in marked reduction of the rat ventral prostate weight. After 7, 14 and 21 days, the prostatic weight was 20%, 11% and 9% of that found for the prostate in non-castrated rats (Fig. 1A). The HA content in the rat ventral prostate was determined by a competitive binding assay using biotinylated HA probe. Figure 1B shows the concentration (mg/g of dry tissue) of HA in prostate of non-castrated and castrated rats. It was shown that castration resulted in higher concentrations of HA in the prostate, with a peak at 14 days. As observed in Fig. 1D, there was a percent variation of 90%, 275% and 85%, for the 7, 14 and 21 days, after castration. On the other hand, the absolute amount of HA in the ventral prostate was reduced after castration. The mean value of 20 μg HA per prostate was reduced to about 9 μg HA per prostate at the 7 and 14 days and to just 5 μg per prostate at 21 days after castration (Fig. 1C). Figure 1D shows that the absolute amount of HA in the ventral prostate of castrated animals is far bellow the non-castrated levels, corresponding to about 40% at days 7 and 14, and only 23.5% at day 21.

Variation in HA chain length

The relative length of the HA chains in the ventral prostate and the variation caused by castration was determined by gel exclusion chromatography. There was a wide range of size distribution, as seen in the representative chromatography shown in Figure 2. We divided the chromatography according to three size range (long, medium and short) and integrated the amount of HA in each of them. It was then observed the predominance of the medium sized chains the non-castrated group. Castration resulted in a transient increase of

the high molecular mass HA (long chains) at 7days after castration and a progressive increase of the low molecular mass HA (short chains) up to 21 days (Fig. 2B). When the absolute amount of HA in the prostate was considered, we noted a decrease in long and medium size classes, most markedly of the medium sized molecules and a slightly increase of short chains after 21 days (Fig. 2C).

HA localization

HA localization was carried out using FITC-labeled HA probe. HA was found in all experimental groups. It showed a uniform distribution in the stroma, but was excluded from blood and lymph vessels. HA was concentrated at the base of the epithelial structures (acini and ducts), around the smooth muscle cells. In the prostate of non-castrated rats (Fig. 3A), a clear labeling of the spaces between the basolateral surface of the epithelium and the basement membrane was observed. HA occupies this space and is retained at the point of tight junctions, close to the apical surface of the cells. Castration resulted in a more compact distribution of HA (Figs. 3C-E). As the epithelium regresses, epithelial labeling was also reduced and less distinct. Some particulate staining was seen and may reflect lysosomal compartmentalization. In the castrated animals, HA distribution was more restricted to the area around the epithelial structures, concentrating around the smooth muscle cells. Previous treatment with bacterial hyaluronidase abolished staining (Fig. 3F).

HAS2 and Hyal1 in situ hybridization

HAS2 biotinylated probe was applied to frozen sections overnight and the hybridization was detected using ABC kit (Figure 4). Staining for HAS2 was weak in the prostate of non-castrated animals, with labeling concentrated in the epithelial and a few stromal cells (Fig. 4A). Castration apparently resulted in wider distribution of HAS2 mRNA labeling in the stroma. However, neither smooth muscle cells nor endothelial cells expressed HAS2 mRNA. After 21 days, the epithelial cells showed decreased staining.

In non-castrated rats, both epithelial and stromal cells are labeled with the probe for the Hyal1 mRNA (Fig. 4E). Epithelial cells showed positive reaction mostly at the basal region, around the cell nucleus. In the stroma, different cells were labeled, but the staining

of perivascular cells was markedly intense. Castration resulted in epithelial regression, but staining for Hyal1 mRNA was still observed (Figs. 4F-H). Castration resulted in progressively denser stroma and progressively denser Hyal1 mRNA labeling. The smooth muscle cells showed reduced labeling, indicating little participation of these cells in hyaluronidase expression and HA degradation.

HAS2 and Hyal1 mRNA expression

Amplification pattern of HAS2, HYAL1 and β-actin cDNA by PCR can be seen in Fig. 5. The results of amplification ratios (Fig. 5B) show that HAS2 mRNA varied but showed no definite tendency within the time line of the experiment. Hyal1 mRNA, on the other hand, showed statistically significant increased expression at days 14 and 21 (Fig. 5C). At this latter point, expression was 2.2-fold higher than the control.

Zymography

Protein extracts from the prostate of non-castrated and castrated rats were electrophoresed in a HA polyacrylamide gel and, after incubation at pH 3.7. The gel was stained with alcian blue and the hyaluronidase activity was observed as a transparent band against a stained background. Figure 6 shows that one main band with hyaluronidase activity was detected in the prostate extracts. In this experiment, the activity of this acidic hyaluronidase decreased progressively after castration, apparently demonstrating a reduction in lysosomal hyaluronidase activity.

CD44 localization

Polyclonal anti-CD44 was applied to frozen sections previously blocked and the signal was revealed by DAB reaction (Fig. 7). Immunohistochemistry of CD44 showed that epithelial cells are predominantly stained in the prostate of both non-castrated (Fig. 7A) and castrated rats (Figs. 7B-D). The apical surface of the epithelial cells was preferentially labeled in the prostate of non-castrated animals. Perivascular cells also showed reactivity for CD44. The reaction observed in the epithelium is apparently stronger and more uniform after castration. In the stroma, endothelial cells and mast cells were positive for CD44. Smooth

muscle cells presented weak surface reaction. Negative controls exhibited no reaction (Fig. 7E).

Discussion

It has been reported that HA concentration in the rat ventral prostate increases after castration (Kofoed et al., 1990; Terry and Clark, 1996). However, as castration results in a marked reduction of prostatic weight this higher concentration does not necessarily imply in higher amount of HA in the prostate. We extended the analysis of the prostatic HA by examining the relative chain length by gel exclusion chromatography, and observed a transient increase in the proportion of long chain molecules at the 7^{th} day after castration and a progressive increase in the short chain molecules up to the 21^{st} day after castration. The most striking observation was the expressive decrease in medium sized molecules. This series of results suggest the predominance of a degradation activity triggered by castration.

We have shown here that HA was distributed in both epithelial and stromal compartments of the prostate gland. The presence of HA in the epithelium could be anticipated, since HA is an important product of keratinocytes. Indeed, it has been calculated that HA concentration in the intercellular space in the epidermis is extremely high, as compared to other tissues (Agren et al., 1995). The presence of HA in the space between the basement membrane and the cell junctions close to the apical surface suggests that the epithelial cells are able to synthesize HA, since it is thought that HA could not cross the basal lamina. It is interesting to observe the presence of HA in the normal epithelium of the prostate, because it has long been known that some cultured prostatic cancer cells, including PC3 cell line produce a HA coat in culture (Simpson et al., 2002b), while others, like LNCaP, do not. It is now possible to conclude that non-tumor prostatic epithelial cells are able to produce HA.

It is tempting to make a correlation between the epithelial disorganization observed in high grade tumors and the increased amount of HA in the plasma. It is well possible that

similarly to PSA, the plasma HA is a result from the non-retained HA production by the prostatic epithelial cells.

On the other hand, it seems that the distribution of HA in the stroma is not changed, thought it shows a different aspect (more granular or interrupted pattern). This pattern seems to result from the rearrangement of smooth muscle cells (which adopts a spinous outline) and collagen fibers (which become convoluted) after castration (Vilamaior et al., 2000), resulting in shorter spaces for the confinement of HA. A more granular aspect of HA in the epithelium in castrated animals may represent a lysosomal location. The use of specific markers for this organelle in double labeling experiments may clarify this matter.

It also worth mentioning that besides epithelial expression, stromal cells also contribute to HA synthesis. Among them, HAS2 mRNA was minimally expressed by smooth muscle cells and endothelial cells, but predominated in other non-identified stromal cells.

We have concentrated our analysis in the expression of HAS2, because the gene coding for this enzyme is located in a chromosomal region (8q24), which is minimally overexpressed in prostatic tumors and may influence tumor development, in conjunct to other genes as c-myc (Tsuchyia et al., 2002). The real time PCR experiment revealed a fluctuation in the mRNA levels for this enzyme after castration, with no defined tendency within the time line of the present experiment. Sustained HAS2 mRNA may be necessary for the maintenance of HA turnover. However, HA synthesis may depend on the activity of two other hyaluronan synthases not analyzed in the work.

Real time PCR also showed a progressively higher expression of Hyal1 after castration. The increased expression of the Hyal1 mRNA may correlate very fine with the overall decrease in the HA content in the whole gland. It is also interesting to mention that Hyal1 is the plasma hyaluronidase and its expression in the prostate may indicate a higher contribution of this organ to the increased amount of this enzyme in the plasma of cancer patients. Besides, we have observed a reduction in lysosomal hyaluronidase activity, using the zymograph at acidic pH. This indicates that HA degradation takes place mostly at the extracellular space.

CD44 immunoreactivity was difuse in the epithelial cells of the prostate in non-castrated. The staining pattern changed after castration, with a more intense staining which concentrated in the apical surface of the epithelium. It seems that this change in epithelial distribution of CD44 is correlated with the population of epithelial cells that survive androgen deprivation. It is well known that basal epithelial cells express CD44 (Liu et al., 1997). This may indicate a predominance of basal (or at least less differentiated epithelial cells) in the prostate of castrated animals. The meaning of CD44 expression on the luminal surface is however unknown.

Finally, it is concluded that the total amount and length of HA chains in the rat ventral prostate is reduced after castration and this is a result of a sustained HAS2 mRNA expression and an increased Hyal1 expression. It was also shown that both epithelium and stroma contribute to the total content of HA in the prostate, but the expression of HA in castrated animals is a major contribution of the stroma.

References

Aaltomaa, S., Lipponen, P., Tammi, R., Tammi, M., Viitanen, J., Kankkunen, J.P., Kosma, V.M. Strong Stromal Hyaluronan Expression Is Associated with PSA Recurrence in Local Prostate Cancer. Urol Int 69: 266-272, 2002.

Agren, U.M., Tammi, M., Tammi, R. Hydrocortisone regulation of hyaluronan metabolism in human skin organ culture. J. Cell. Physiol. 164: 240-248, 1995.

Bustin, S.A. Absolute quantification of mRNA using real-time reverse transcription polymerase chain reactions assay. J. Mol. Endocrinol. 25: 169-193, 2000.

Carvalho, H.F., Line, S.R.P. Basement membrane associated chances in the rat ventral prostate following castration. Cell Biol. Int. 20: 809-819, 1996.

Carvalho, H.F., Vilamaior, P.S.L., Taboga, S.R Elastic system of the rat ventral prostate and its modifications following orchiectomy. Prostate 32: 27-34, 1997a.

Carvalho, H.F., Taboga, S.R., Vilamaior, P.S.L. Collagen type VI is a component of the extracellular matrix microfibrils network of the prostatic stroma. Tissue Cell 29: 163-170, 1997b.

Deprez, R.H.L., Fijnvandraat, A.C., Ruijter, J.M., Moorman, A.F. Sensitivity and accuracy of quantitative real-time polymerase chain reaction using SYBR Green I dependent on cDNA synthesis conditions. Anal. Biochem. 307: 63-69, 2002.

Fraser, J.R., Laurent, T.C., Laurent, U.B. Hyaluronan: its nature, distribution, functions and turnover. J. Intern. Med. 242: 27-33, 1997

Higuchi, R., Fickler, C., Dollinger, G., Watson, R. Kinetic PCR analysis: real-time monitoring of cDNA amplification reactions. Biotechnology 11:1026-1030, 1993.

Kofoed, J.A., Tumilasci, O.R., Curbelo, H.M. Fernadez Lemos, S.M., Arias, N.H., Houssay, A.B. Effects of castration and androgens upon prostatic proteoglycans in rats. Prostate 16: 93-102, 1990.

Laurent, T.C., Fraser, J.R. Hyaluronan. FASEB J. 6: 2397-2404, 1992.

Li Y, Rahmanian M, Widström C, Lepperdinger G, Frost GI & Heldin P. Irradiation-induced expression of hyaluronan (HA) synthase 2 and hyaluronidase genes in rat lung tissue accompanies active turnover of HA and inductionof types I and III collagen gene expression. Am. J. Resp. Cell. Mol. Biol. 23: 411-418,2000.

Liu, A.Y., True, L.D., LaTray, L., Nelson, P.S., Ellis, W.J., Vessella, R.L., Lange, P.H., Hood, L,, van den Engh, G. Cell-cell interaction in prostate gene regulation and cytodifferentiation. Proc. Natl. Acad. Sci. USA 94: 10705-10710, 1997.

Lokeshwar, V.B., Obek, C., Soloway, M.S., Block, N.L. Tumor-associated hyaluronic acid: a new sensitive and specific urine marker for bladder cancer. Cancer Res. 57: 773-777, 1997.

Lokeshwar, V., Rubinowicz, D. Hyaluronic acid and hyaluronidase: molecular markers associated with prostate cancer biology and detection. Prostate Cancer. Prostatic. Dis. 2(S3): S21, 1999

Meijerink, J., Mandigers, C., van de Locht, L., Tonnissen, E., Goodsaid, F., Raemaekers, J. A novel method to compensate for different amplification efficiences between patient DNA samples in quantitative real-time PCR. J. Mol. Diagn. 3: 55-61, 2001.

Pfaffi, M.W. A new mathematical model for relative quantification in real-time RT-PCR. Nucl. Acids Res. 29: e45, 2001.

Simpson, M.A., Wilson, C.M., McCarthy, J.B. Inhibition of prostate tumor cell hyaluronan synthesis impairs subcutaneous growth and vascularization in immunocompromised mice. Am. J. Pathol. 161: 849-857, 2002a.

Simpson, M.A., Wilson, C.M., Furcht, L.T., Spicer, A.P., Oegema Jr, T.R., McCarthy, J.B. Manipulation of hyaluronan synthase expression in prostate adenocarcinoma cells alters pericellular matrix retention and adhesion to bone marrow endothelial cells. J. Biol. Chem. 277: 10050-10057, 2002b.

Tengblad, A. Affinity chromatography on immobilized hyaluronate and its application to the isolation of hyaluronate binding properties from cartilage. Biochim. Biophys. Acta 578:281-289, 1979.

Terry, D.E., Clark, A.F. Glycosaminoglycans in the three lobes of the rat prostate following castration and testosterone treatment. Biochem. Cell Biol. 74:653-658, 1996.

Tsuchiya, N., Kondo, Y., Takahashi, A., Pawar, H., Qian, J., Sato, K., Lieber, M.M., Jenkins, R.B. Mapping and gene expression profile of the minimally overrepresented 8q24 region in prostate cancer. Am. J. Pathol. 160: 1799-1806, 2002.

Vilamaior, P.S.L., Felisbino, S.L., Taboga, S.R., Carvalho, H.F. Collagen fiber reorganization in the rat ventral prostate following androgen deprivation: a possible role for smooth muscle cells. Prostate 45: 253-258, 2000.

Legends of the figures

Figure 1. Variation in the rat ventral prostate weight and HA after castration. Fig. 1A depicts the ventral prostate weight reduction as attained by castration. After 7, 14 and 21 days, the prostatic weight corresponded to 20%, 11% and 9% of the control value, respectively. Fig. 1B. shows the concentration of HA in the prostate at the different experimental situations. There is an increment in the concentration of HA in the prostate of castrated rats, with a peak at 14 days after castration. The absolute amount of HA per prostate (Fig. 1C), however, decreased after castration, from the mean of 20 μg of HA per prostate in the non-castrated rats, to about 9 μg at days 7 and 14 after castration, and 5μg at day 21. Figure 1D represents the percent variation of the concentration of HA and the absolute amount of HA per prostate. The control values for each variable was set as 100%.

Figure 2. HA chain size variation. The hydrodynamic size of the HA chains in the prostate of non-castrated and castrated rats was determined by gel exclusion chromatography in a Sepharose CL6B column. Figure 2A shows a representative chromatogram obtained for the HA extracted from the prostate of a castrated animal, 7 days after castration. The size distribution was wide. The fractions were divided in three groups, with Kav varying from 0.1 and 0.3; 0.35 and 0.7, and 0.74-1.0. The HA content in each of these size groups was determined by integration of the peaks. Figure 2B reveals the percentual of HA in each fraction for the different experimental points. It is noted an increase in the proportion of high size molecules 7 days after castration and a progressively increment in the low size molecules. In figure 2C, the absolute amount of HA in each situation was considered so that an overall reduction in the amount of HA is made clear. In this graph one can see that the most marked changes is a reduction in the medium sized chains, followed by a discrete increment in the low sized chains.

Figure 3. HA localization in the rat ventral prostate. HA was localized using a FITC-labeled probe. HA was distributed in both epithelial and stromal compartments of the

prostate of non-castrated (Fig. 3A,B) and castrated animals (Fig. 3C-E). In the prostate of non-castrated rats, HA labeling was intense at the base of the epithelium, and among the smooth muscle cells. In the epithelial compartment, HA was found between the epithelial cells up to the point of tight junctions. In the stroma, cells and fibers excluded HA and appeared unstained. Castration resulted in collapse of the pattern observed in the control. HA was still found in the epithelium and stroma, but showed a more particulate staining, what it thought to be due to the new distribution of HA around the newly arranged cells and fibers. It seems that some intracellular granules could correspond to lysosomes. The pattern observed for the castrated rats was maintained for the 7- (Fig. 3C), 14- (Fig. 3D) and 21-day (Fig. 3E) time points. Figure 3F is a control section treated with bacterial hyaluronidase before incubation with the HA probe and nuclei were DAPI stained. Ep = epithelium; st = stroma. Bars (1.1cm) = 25 μm (A, C-E) and 10 μm (B, F).

Figure 4. In situ hybridization for HAS2 and Hyal1. The HAS2 mRNA was found in the epithelial and some stromal cells. No reaction was observed in endothelial cells, but perivascular cells expressed the HAS2 mRNA (Fig. 4A). Castration did not change the expression pattern of the epithelium (ep) (Figs. 4B-D). However, there was a more defined compartmentalization of HAS2 expression in the stroma (st). The smooth muscle cells (smc) and endothelial cells showed very weak, if any, reaction, while other stromal cells showed more intense reaction. The in situ hybridization reaction for Hyal1 was demonstrated in the epithelium and in the stroma. Endothelial cells were negative. Positive and negative cells were observed in the stroma of non-castrated rats (Fig. 4E). The Hyal1 mRNA expression by the epithelium was not changed by castration (Figs. 4F-H), though seemed slightly lower after 21 days. As for HAS2, the stromal expression of Hyal1 was more compartmentalized, with very weak reaction in the smooth muscle cells and more intense reaction in other stromal cells. A and E, non-castrated rats; B and F, 7 days after castration; C and G, 14 days after castration; D and H, 21 days after castration. v = blood vessel. Bars (1.1 cm) = 25 μm.

Figure 5. HAS2 and Hyal1 mRNA expression levels in the prostate. Real time PCR was employed for the determination of the HAS2 and Hyal1 mRNA expression in the rat ventral prostate. Figure 5A is the amplification pattern obtained for the endogenous standard, β-actin, HAS2 and Hyal1. β-actin mRNA was employed for the sake of comparison between the samples. Figures 5B and 5C show the fold change obtained for HAS2 and Hyal1, respectively. It was observed that the expression level of HAS2 varied along the time line of the experiment, but showed no specific tendency. Hyal1 mRNA expression, however, showed a progressively increased expression, reaching more than twice mRNA expression as compared to the prostate of non-castrated rats.

Figure 6. Hyaluronidase zymography. Analysis of the hyaluronidase activity using zymography shows a main band of acidic hyaluronidase activity (pH 3.7) (Fig. 6A). Castration resulted in a reduction of the intensity of the hyaluronidase activity, as confirmed by densitometry of the bands (Fig. 6B). Seven days after castration there was a 40% reduction, which increased a little further, reaching 40% reduction at the 14 and 21 days after castration.

Figure 7. CD44 localization in the prostate. Immunocytochemistry revealed the presence of CD44 in the epithelial cell (ep), as well as some stromal cells, including blood vessel (v) lining endothelial cells (Fig. 7A). Castration did not abolished the same pattern of CD44 distribution (Fig. 7B-D), however, labeling of the epithelial cell surface was more intense. B, C and D, 7, 14 and 21 days after castration. Fig. 7E, negative control. v = blood vessel. Bars (1.1 cm) = 25 μm.

Figure 1

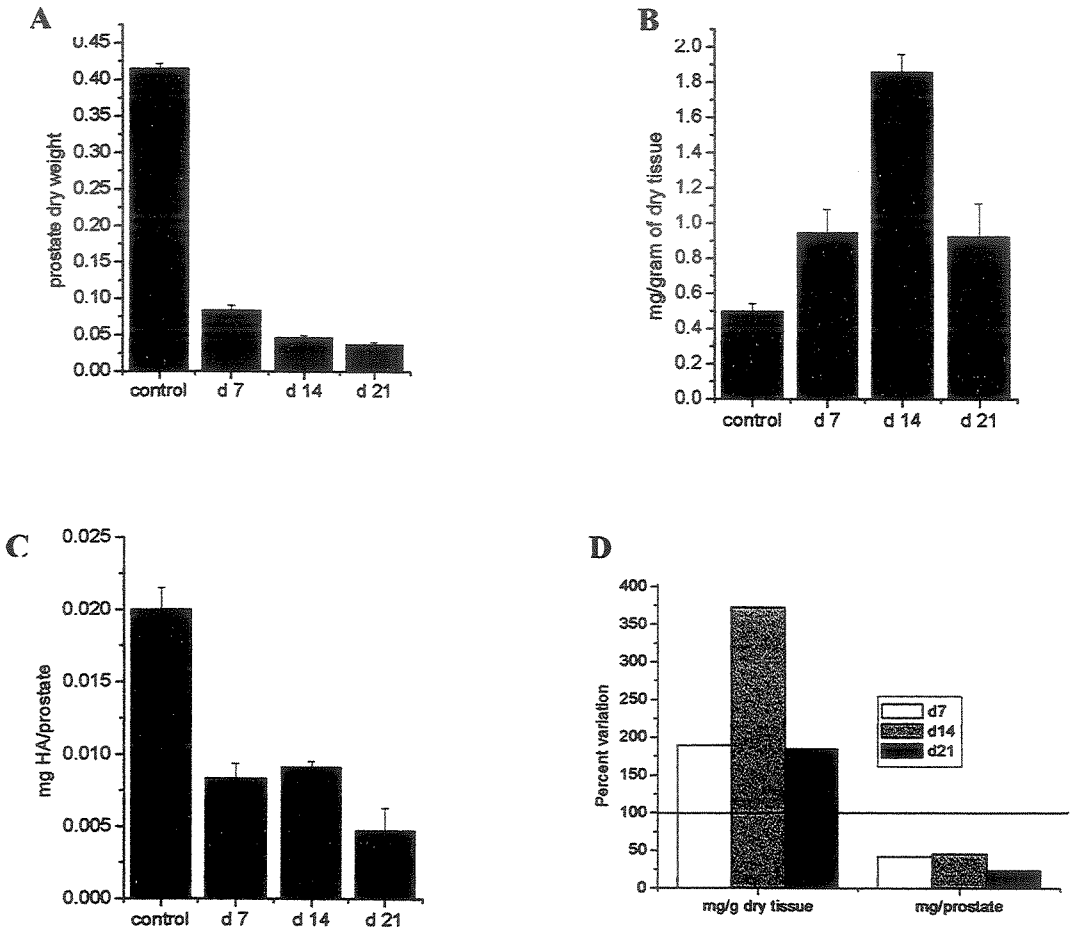
A
prostate dry weight
0.45
0.40
0.35
0.30
0.25
0.20
0.15
0.10
0.05
0.00
control
d 7
d 14
d 21
B
mg/gram of dry tissue
2.0
1.8
1.6
1.4
1.2
1.0
0.8
0.6
0.4
0.2
0.0
control
d 7
d 14
d 21
C
mg HA/prostate
0.025
0.020
0.015
0.010
0.005
0.000
control
d 7
d 14
d 21
D
Percent variation
400
350
300
250
200
150
100
50
0
d7
d14
d21
mg/g dry tissue
mg/prostate

Figure 2

A

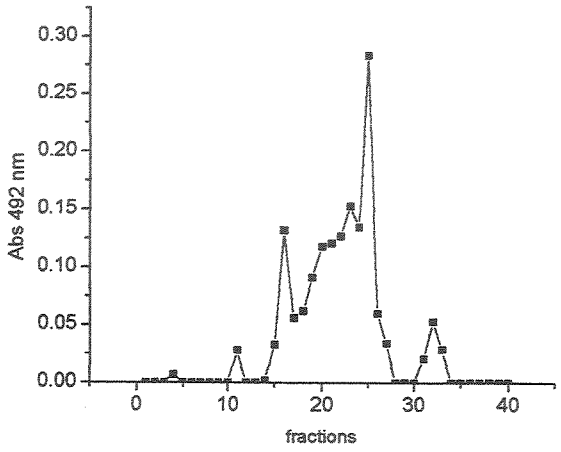
0.30
0.25
0.20
0.15
0.10
0.05
0.00
Abs 492 nm
0
10
20
30
40
fractions

B

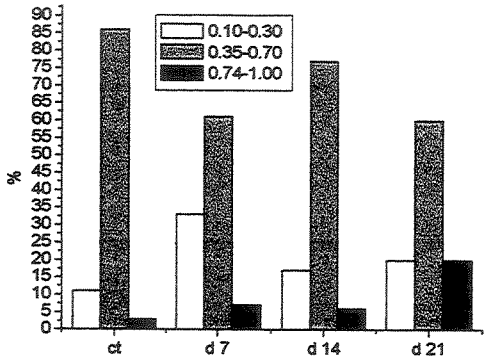
0.10-0.30
0.35-0.70
0.74-1.00
%
ct
d 7
d 14
d 21

C

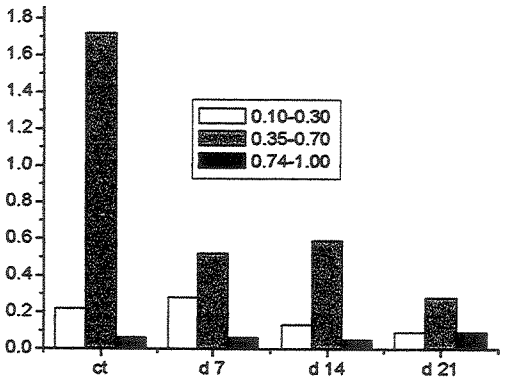
0.10-0.30
0.35-0.70
0.74-1.00
ct
d 7
d 14
d 21

Figure 3

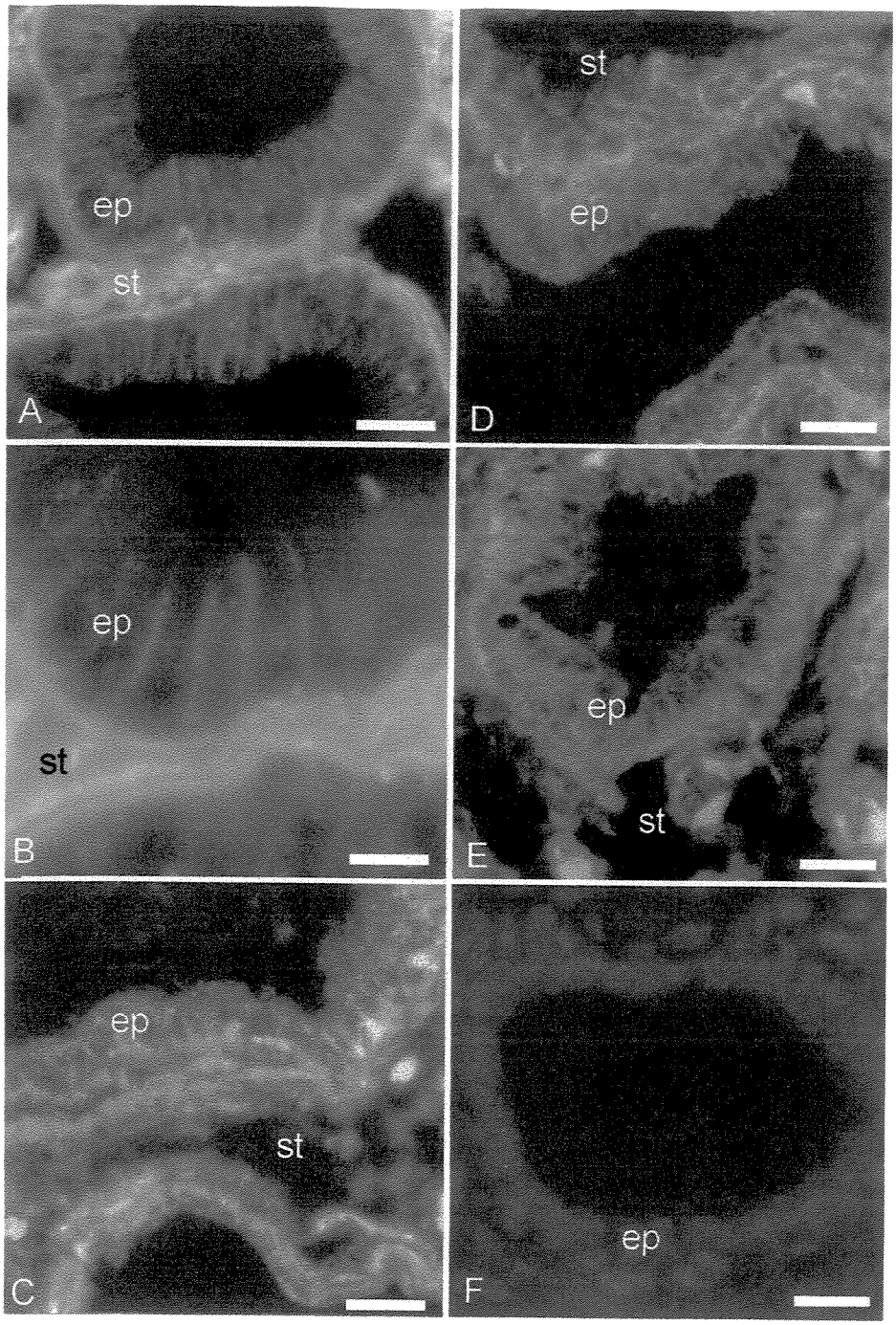

Figure 4

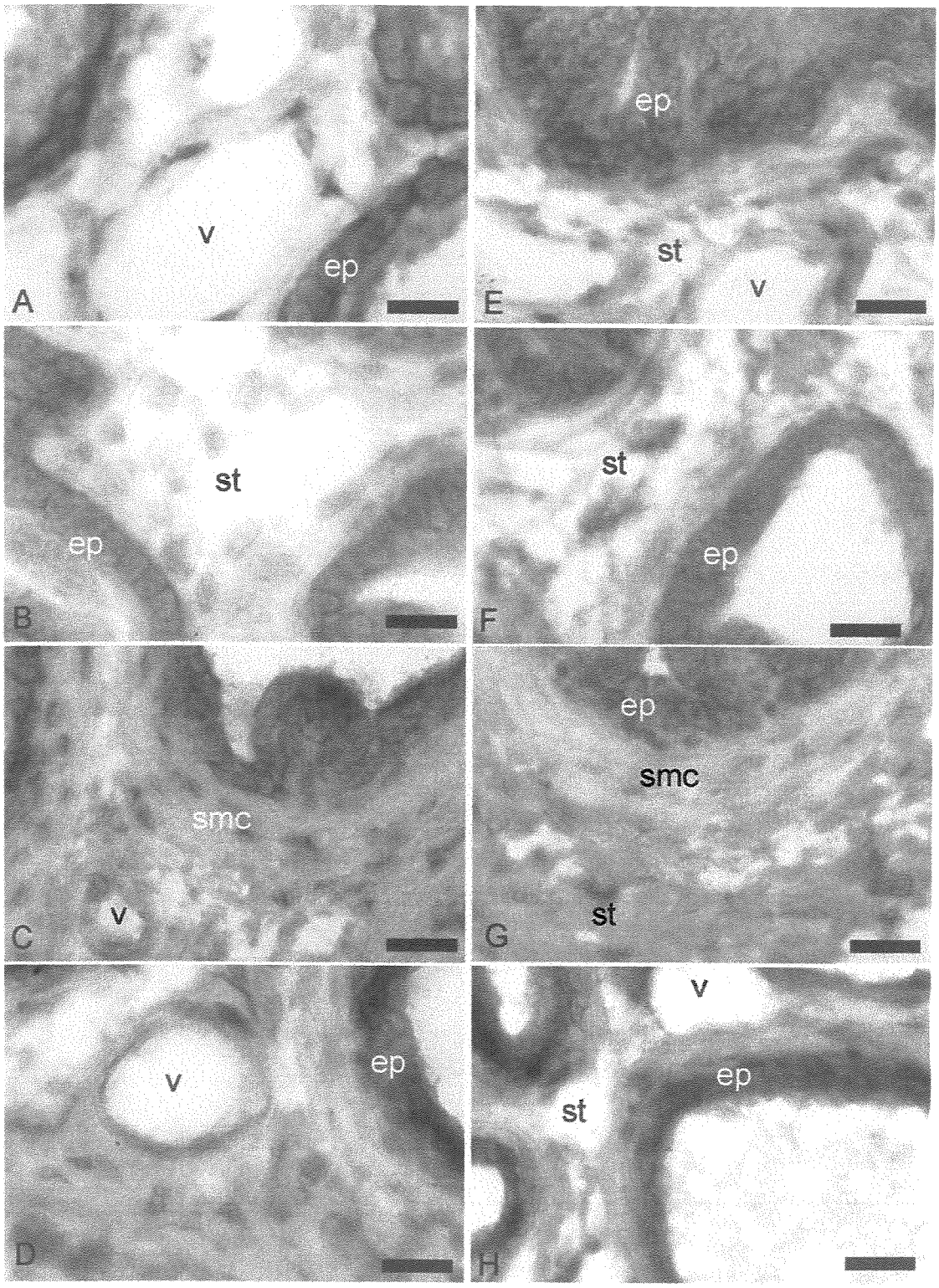

Figure 5

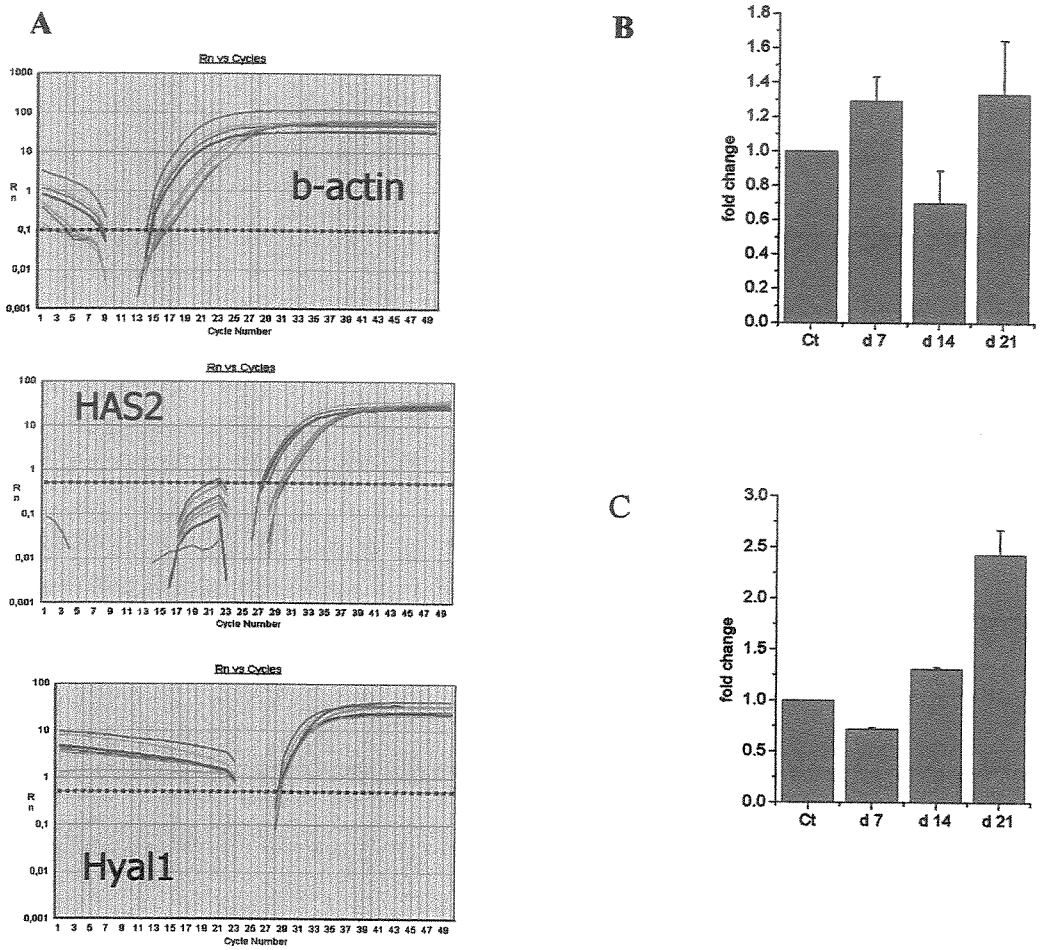
A
Rn vs Cycles
b-actin
Cycle Number
Rn vs Cycles
HAS2
Cycle Number
Rn vs Cycles
Hyal1
Cycle Number
B
fold change
Ct
d 7
d 14
d 21
C
fold change
Ct
d 7
d 14
d 21

Figure 6

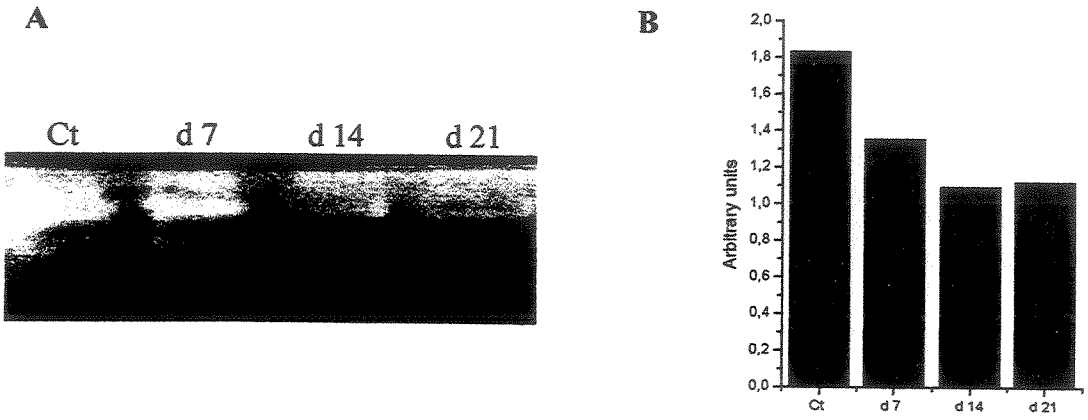
A
Ct
d 7
d 14
d 21
B
Arbitrary units
2,0
1,8
1,6
1,4
1,2
1,0
0,8
0,6
0,4
0,2
0,0
Ct
d 7
d 14
d 21

Figure 7

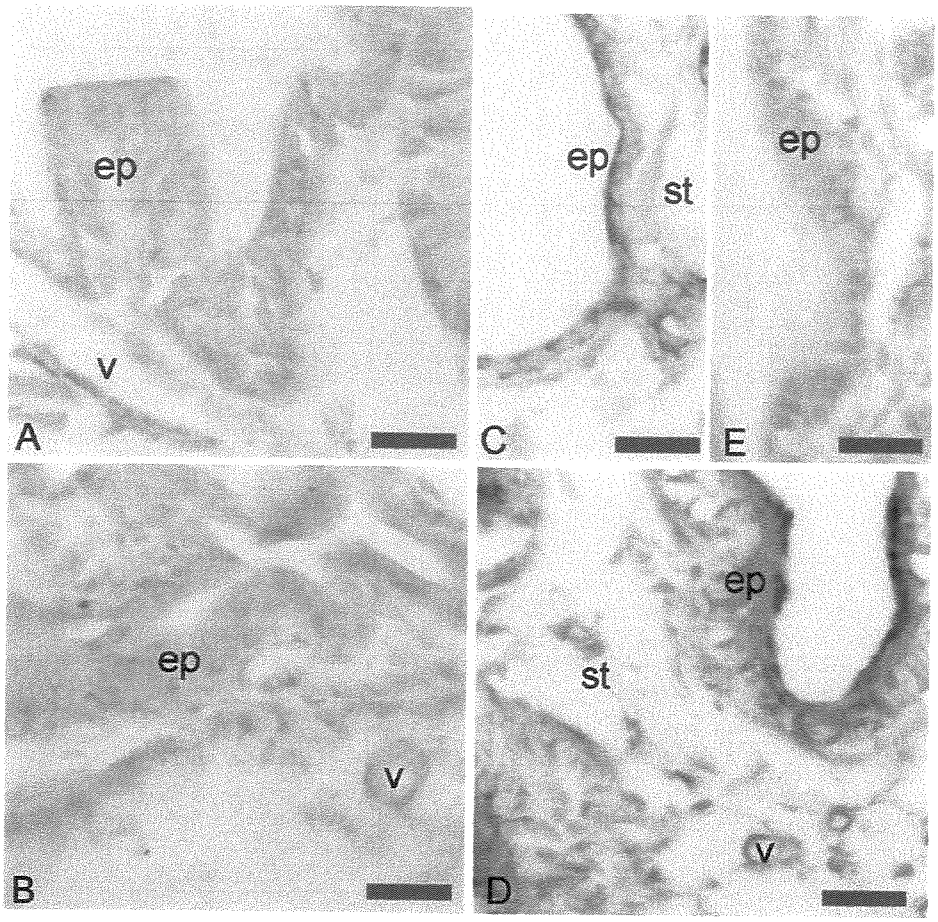

Artigo 2

Culturing rat prostatic smooth muscle cells: Maintenance of the differentiated state and hyaluronan synthesis

Submetido a Biochemistry and Cell Biology

Culturing rat prostatic smooth muscle cells:

Maintenance of the differentiated state and hyaluronan synthesis

Heloisa H. M. Della Colleta, Eliane Antonioli, Hernandes F Carvalho

Department of Cell Biology, Institute of Biology - State University of Campinas – UNICAMP

Campinas SP, Brazil

Corresponding author: Hernandes F Carvalho

Department of Cell Biology – UNICAMP

CP6109

13083-063 Campinas SP, Brazil

Tel. 55 19 3788 6118

Fax 55 19 3788 6111

E-mail hern@unicamp.br

Running header: Prostatic smooth muscle cells in culture

Summary

Smooth muscle cells (SMC) are important components of the prostatic stroma and are involved in diverse phenomena such as organ development, homeostasis and stromal reorganization under androgen deprivation. In this work we have studied the differentiation status and ability to synthesize hyaluronan (HA) of rat prostatic smooth muscle cells in vitro up to passage 8 in the presence of testosterone and insulin. Expression of smoothelin, SM22 and calponin was detected at the mRNA level along the 8 passages, indicating the maintenance of the differentiated state. On the other hand, cells were demonstrated to synthesize HA both as a cell coat and as secreted component of the culture medium. HA concentration in the medium droped up to passage 4 and raised again to the initial levels at passage 5, to drop again up to passage 8. The cell coat also varied, but was almost absent during passages 1, 2 and 3, and tend to increase after passage 4. We conclude that smooth muscle cells can be maintained in the differentiated state in culture and that these cells produce HA at variable amounts after different passages.

Key-words: smooth muscle cell, calponin, SM22, smoothelin, hyaluronan, prostate

1. Intoduction

Stroma-epithelial interactions are instructive during prostate development (Thomson et al., 2002) and important for the function of the organ in the adult stage. Among the prostatic stromal cells, smooth muscle cells (SMC) are thought to play important roles in the maintenance of the epithelial physiology and survival (Kurita et al., 2001; Tuxhorn et al., 2001; Thomson et al., 2002). The SMC also exhibit considerable plasticity in their response to a variety of physiological stimuli (Owens, 1995; Tuxhorn et al., 2001). Furthermore, it has been pointed out that SMC may exert key functions during the development of prostatic cancer and were suggested to take part in the stromal reaction during cancer invasion (Hayward et al., 1996, Cunha et al., 1996; Hayward et al., 1997; Tuxhorn et al., 2001).

A central point in the biology of the SMC in this stromal reaction is the preservation of the differentiated state. Tuxhorn et al. (2001; 2002) and Ayala et al. (2003) have suggested that SMC are displaced by myofibroblasts or switch from a quiescent contractile phenotype to a proliferative synthetic phenotype, which also shows the features of myofibroblasts.

Castration also results in modifications of the SMC phenotype. The cells adopt an irregular outline and occupy a higher volume of the prostatic stroma (Antonioli et al., 2004). Previous work has suggested that SMC dedifferentiated after long-term castration (Hayward et al., 1996). However, we have shown that SMC in the prostate of castrated rats still express smoothelin in addition to smooth muscle specific myosin heavy chain, suggesting that, at least within a 21 days time line, the SMC are still in the differentiated state. We have then suggested that prostatic SMC shift phenotype after castration, without loosing the differentiated state, and are actively involved in the stromal remodeling taking place under androgen deprivation. Amongst the stromal modification there is an increase of hyaluronan concentration (Kofoed et al., 1990). Such modification is also a key event of the stromal reorganization during tumor invasion (Lokeshwar et al., 2001).

In this work we decided to culture rat prostatic SMC to follow the expression of a series of differentiation markers (Dovendans & Van Eys, 2002) along culture passages, to verify whether they maintain the differentiated state in vitro. Furthermore, we have also

checked the ability of SMC to synthesize hyaluronan, by quantitating its amount in the culture medium and the size of the HA coat and the CD44 localization.

The results demonstrated that the rat SMC maintain their differentiated state in culture as well as are able to produce and assemble a HA coat, which varied with time in culture.

2. Materials and Methods

2.1. Primary Prostatic SMC Culture

Smooth muscle cells were prepared using a modification of the protocol described by Gerdes et al. (1996). In brief, the ventral prostate of young adult Wistar rats was minced into 1-2 mm^3 fragments and placed in DMEM (Nutricell, Campinas SP, Brazil) supplemented with 10% fetal calf serum (FCS), 1% penicillin/streptomycin solution, 5 μg of insulin/mL (BioBrás, Belo Horizonte MG, Brazil) and 0.5 μg of testosterone ciprionate/mL (Novaquímica – Sigma Pharma, Hortolândia SP, Brazil) in 24-well culture plates. The medium was replaced every 48 h.

After reaching 80% confluence, SMC were replated using trypsin/EDTA (Nutricell) and cultured in 25 cm^2 culture flasks at 37°C in a humidified atmosphere with 5% CO_2. Cells were maintained until passage 8. Passage 0 refers to cells that just migrated out of the explant and adhered to the plate, before subculturing. In another series of experiments, cells in passage 6 were cultured with either testosterone or insulin or with no added hormone, for 96hs, including a subculturing at 48 hs.

2.2. Immunocytochemistry

Immunocytochemical staining of the cultures was used to characterize the cells. SMC were plated on coverslips in 24-well plates (2×10^4 cells/well), cultured for 24 h and fixed in 4% formalin. Monoclonal antibodies against α-smooth muscle actin (Sigma Chemical Co., St. Louis, MO), smooth muscle myosin heavy chain (SM-MHC) and CD44 (Santa Cruz Biotech, Santa Cruz CA) were used. For α-smooth muscle actin and SM-MHC, primary

antibodies were diluted in a solution of 1% bovine serum albumin (BSA) in Tris-buffered saline containing 0.1% Tween 20 (TBS-T), according to the manufacturer's instructions, and applied to the cells overnight at 4°C. After three 5 min washes with TBS-T, the cells were incubated with a secondary fluorescein-conjugated antibody against mouse polyvalent immunoglobulins (Sigma Chemical Co.) (diluted 1:120) in 1% BSA in TBS-T. Coverslips were mounted in a DABCO (Sigma Chemical Co.) solution containing 5 μM DAPI (Sigma Chemical Co.).

For CD44 primary antibody, previously endogenous peroxidase was blocked by incubating the coverslips with 3% H_2O_2 (in water) for 20 min. Non-specific protein binding was blocked with 3% BSA in TBS-T. The coverslips were incubated with the primary antibody diluted in 1% BSA overnight at 4°C. The slides were washed with TBS-T and incubated with HRP-labeled anti rabbit Ig antibody for 2 hours at room temperature. The coverslips were washed with TBS-T and developed with 0.05% 3, 3′-diaminobenzidine tetrahydrochloride and 0.03% hydrogen peroxide in phosphate buffer (0.05 M, pH 7.4) at room temperature. The coverslips were air dried and mounted in Entellan. Negative controls were obtained by omitting the incubation with the primary antibody. Observations were made using a Olympus BX60 microscope and photographs were taken using Kodak 400 Pro-image film.

Alternatively, cells were stained with rhodamin-labeled phalloidin (Sigma Chemical Co. (Saint Louis MO, USA), before examination under the green light excitation in a Zeiss Axioskop fluorescence microscope.

2.3. RT-PCR

RNA was isolated from cells in each passage. The cells were incubated with TRIzol reagent (Invitrogen Life Technologies, Carlsbad CA, USA) and the extraction procedures were made according to manufacturer. Five-microgram of RNA was subjected to reverse transcription using SuperScript III (Invitrogen Life Technologies). The cDNA obtained was used in PCR experiments. PCR oligonucleotides specific for smoothelin (sense 5'-GTCGACATCCAGAACTTCCTCC-3'; antisense 5'-CGCAGGTGGTTGTACAGCGA-3'), calponin (sense 5'-GAAGATCAATGAGTCAACCC-3'; antisense 5'-

TGTTCTCAAACAGGTCGTTGGC-3'), SM22 (sense 5'-AGGTCTGGCTGAAGAATGGC-3'; antisense 5'-TTCAAAGAGGTCAACAGTCTGG-3') and β-actin (sense 5'-TCACCCACACTGTGCCCATCTACGA-3'; antisense 5'-CAGCGGAACCGCTCATTGCCAATGG3') were used. Expected products sizes were 450 bp (visceral) and 300 bp (vascular) for smoothelin, 125 bp for calponin, 200 bp for SM22 and 310 bp for β-actin. Cycling conditions were optimized independently. Annealing temperature varies according each primer: 54°C for smoothelin, 53°C for calponin, 59.5°C for SM22 and 60°C for β-actin. In brief, cycles were 5 min of initial denaturation; 30 cycles of 30 sec 94°C, 30 sec annealing temperature and 1 min 72°C; 7 min at 72°C to a final extension. Smoothelin presented different cycles: 2 min at 94°C, 35 cycles of 30 sec 94°C, 30 sec 54°C and 30 sec 72°C with 5 min at 72°C to a final extension. Prostate was used as positive control and LNCaP and PC3 cells were used as negative control.

2.4. HA quantitation

The cells were cultured by 48 hours and the medium was replaced by fresh medium without FBS in each passage. After 24 hours, the medium was collected and the concentration of HA in culture medium of cells was determined in a competitive binding assay (Lokeshwar et al., 1997). Briefly, 100 μL of sera samples or standard concentrations of HA (Sigma) diluted in assay buffer (0.05M Tris-HCl, 0.15M NaCl, 0.05% Tween 20, 0.0074 g/L EDTA III, 0.5 g/L sodium azide, BSA 1%, pH 7.75) are added, in triplicate, to FluoroNUNC Maxisorp-microplates Roskilde, Denmark) previously coated with HA-binding protein. After an overnight incubation, the plates are washed with washing buffer (0.05 M Tris-HCl, 0.15 M NaCl, 0.05% Tween 20, 0.074 g/L EDTA III, 0.5 g/L sodium azide, pH 7.75) and sequentially incubated with biotinylated HA-binding protein and europium-labelled streptavidin, purchased from Wallac (Turku, Finland). Afterwards, the europium bound to the solid phase is released by na enhancement solution and the fluorescence measured by a time-resolved fluorometer Victor 2, both solution and equipament from Wallac. The data (counts/s) are then processed automatically in the MultiCalc softwares program from Pharmacia.

The results obtained with cell culture media were expressed in ng/mL of HA according to HA standard concentrations. The values were normalized with protein quantities measured in a Bradford assay kit (BioRad) and the final results are expressed in ng HA/mg protein.

2.5. Particle exclusion assay

Pericellular HA matrices were visualized as described (Knudson & Toole, 1985). Briefly, 2 x 10^4 cells cultured overnight in 24 well plates were washed and fresh medium containing $1x10^8$ glutaraldehyde-fixed sheep red blood cells was added. Red blood cells were settled for 15 min and the cultures then viewed under phase-contrast microscopy. The HA matrix was evidenced by halos surrounding the cells from which the fixed erythrocytes were excluded. Matrix retention was quantified (Simpson et al., 2002) tracing outlines of matrices and cellular boundaries from 10 individual cells of each passage. Areas were measured using a Image J software and relative areas were calculated dividing cell plus coat area per cell area, so that a ratio of 1 indicates complete absence of pericellular halo. Negative controls were made incubating cells with *Streptomyces* hyaluronidase for 30 min prior addition red blood cell suspension.

3. Results

Cultured rat prostatic smooth muscle cells have a roughly rounded outline sub-confluent cultures and fibroblastic morphology at confluency.

Immunocytochemistry revealed a positive reaction for the smooth muscle cell markers α-smooth muscle actin (Fig. 1a) and smooth muscle myosin heavy chain (Fig. 1b). Phalloidin staining revealed an abundant actin-based cytoskeleton forming stress fibers that occupy the cytoplasm thoroughly (Fig. 2).

Further characterization of the SMC was obtained by analysis of the expression of the three smooth muscle specific markers at the mRNA level by RT-PCR. The results showed that smoothelin, SM22 and calponin (markers of the differentiated state of SMC,

according Dovendans & Van Eys, 2002) are expressed by the SMC regardless the subculturing stage up to passage 8 (Fig. 3). Densitometric analysis of the PCR product including normalization with the β-actin amplification product showed very little, if any, variation in the expression levels of the three markers (not shown).

We have used cells at passage 6 to test the effect of insulin and testosterone on the expression of these same SMC markers. Removal of either or both did not affect the expression of smoothelin, SM22 or calponin (Fig. 4).

Quantification of HA in the culture medium revealed a drop in HA concentration up to passage 4 and then a sudden recover at passage 5, followed by a second decrease, similar to the first phase (Fig. 5).

The cultured rat smooth muscle cells assemble a HA coat at the cell surface (Fig. 6a). Quantitative analysis revealed that the size of the coat is variable and almost absent at passages 1, 2 and 3 (Fig. 6b). At passage 5 and thereafter, the wide variation in coat size is recovered, what contributes to an increase in the mean size of the coat.

CD44, the hyaluronan cell surface receptor, was found in all passages studied in work. Staining was found at the cell surface and was visible stronger in dividing cells (Fig. 7a). Cells cultured in the presence of testosterone without insulin, showed an accumulation of CD44 immunoreactitivy at the cell periphery (Fig. 7b).

4. Discussion

The phenotypical plasticity of smooth muscle cells is evident in at least two situations. Castration results in marked morphological alterations of these cells. It was reported before that prostatic SMC undergoes dedifferentiation, as based on the increase expression of vimentin and reduced expression of smooth muscle α-actin (Hayward et al., 1996). We have recently shown that within a 21-day time line, the expression of smooth muscle specific α-actin and myosin heavy chain (at the protein level) and smoothelin (at the mRNA level) are not affected by castration, despite the morphological changes observed, which suggested us that SMC are able to change from a predominantly

contractile phenotype to a so-called synthetic phenotype, without dedifferentiating (Antonioli et al., 2004). Furthermore, at the ultrastructural level, the presence of reduced, but still abundant microfilaments, dense plaques in the cytoplasm and at the cell surface and basement membrane are characteristics of SMC still observed after castration (unpublished results).

SMC plasticity is also observed during tumor invasion. It has been stressed that SMC change phenotype during tumor epithelial cell invasion. The observed changes are included in the stromal reaction, and described as a SMC to myofibroblast transition (Tuxhorn et al., 2001; 2002; Ayala et al., 2003).

We have characterized the rat prostatic SMC in culture. The isolated cells do not assume the classical hill-and-valley arrangement as shown by human prostatic SMC. However, these cells were demonstrated to express smooth muscle specific myosin heavy chain and α-actin by immunocitochemistry and three of the SMC markers: smoothelin, SM22 and calponin, at the mRNA level. Furthermore, we have shown that subculturing does not affect the expression of these markers up to passage 8, although it has been reported that vascular SMC assume a proliferative and synthetic phenotype as described by Rovner et al. (1986).

These results are important because rat SMC may appear as an important model system, avoiding the non-uniformity of samples taken from human patients. We have also shown that insulin and testosterone does not influence the expression of SMC markers within a 96 h culturing.

We have also assessed the ability of the rat SMC to produce HA and to assemble a HA coat. The HA concentration in the culture medium showed a progressive decrease up to passage 4 and then a sudden recover of the value seen at the beginning followed by a second drop. The reason for this pattern of HA expression is currently unknown.

Similarly, the HA completely disappeared at passages 3 and 4. It is possible that the first decrease correspond to an adaptation to the high insulin concentration employed in this culture system, since it was shown before that concentrations above 50 μU causes inhibition of HA production by vascular smooth muscle cells (Erikstrup et al., 2001).

The study of HA production by SMC is important because it seems necessary to understand the relationship between hyaluronan concentration and tumor progression (Lokeshwar & Rubinowicz, 1999; Aaltomaa et al., 2002). In the accompanying paper (Della Colleta et al., 2004) we have observed that in vivo SMC express very little hyaluronan synthase 2 (HAS2) mRNA by in situ hybridization, what may indicate that this cell type is not involved with major of the HA production in the rat prostate in both non-castrated and castrated rats.

The assemble of the HA coat is, at least in part, favored by the expression of the CD44 receptor, which was found to be expressed all over the different passages. It is interesting to note that, in the presence of testosterone alone (i.e. without insulin), CD44 labeling was displaced and accumulated at the cell periphery. This may indicated that cells under this circumstance may adopt a migratory behavior, what will deserve further research in the future.

The present results demonstrate that SMC keep their differentiated phenotype in culture and are able to synthesize and assemble a HA surface coat. The implications of these results are that this culture conditions may be used for the study of factor affecting the differentiation status of SMC and that SMC are at least in part involved with the HA metabolism in the prostate and with the modifications this glycosaminoglycan shows after castration and likely during tumor invasion.

Acknowledgements

The authors are grateful to Dr. Helena B. Nader for allowing the use of facilities in her laboratory for the quantitation of HA.

References

Aaltomaa S., Lipponen P., Tammi R., Tammi M., Viitanen J., Kankkunen J.P. & Kosma V.M. (2002). Strong stromal hyaluronan expression is associated with PSA recurrence in local prostate cancer. *Urology International*, 69: 266-272.

Antonioli E., Della-Colleta H.H.M. & Carvalho H.F. (2004). Smooth muscle cell behavior in the ventral prostate of castrated rats. *Journal of Andrology*, 25: 50-56.

Ayala G., Tuxhorn J.A., Wheeler T.M., Frolov A., Scardino P.T., Ohori M., Wheeler M., Spitler J. & Rowley D.R. (2003). Reactive stroma as a predictor of biochemical-free recurrence in prostate cancer. *Clinical of. Cancer Research*, 9: 4792-4801.

Cunha G.R., Hayard S.W., Dahiya R. & Foster B.A. (1996). Smooth muscle-epithelial interactions in normal and neoplastic prostatic development. *Acta Anatomica*, 155: 63-72.

Della-Colleta H.H.M., Saad S.T. & Carvalho H.F. (2005). Effects of castration on hyaluronan synthesis and degradation in the rat ventral prostate. Submitted.

Doevendans P.A. & Van Eys G. (2002). Smooth muscle cells on the move: the battle for actin. *Cardiovascular Research*, 54: 499-502.

Erikstrup C., Pedersen L.M., Heickendorff L., Ledet T. & Rasmussen L.M. (2001). Production of hyaluronan and chondroitin sulphate proteoglycans from human arterial smooth muscle--the effect of glucose, insulin, IGF-I or growth hormone. *European Journal of Endocrinology*, 145: 193-198.

Gerdes M.J., Dang Truong D., Lu B., Larsen M., McBride L. & Rowley D.R. (1996). Androgen-regulated proliferation and gene transcription in a prostate smooth muscle cell line (PS -1). *Endocrinology*, 137:864-872.

Hayward S.W., Baskin L.S., Haughney P.C., Foster B.A., Cunha A.R., Dahiya R., Prins G.S. & Cunha G.R. (1996). Stromal development in the ventral prostate, anterior prostate and seminal vesicle of the rat. *Acta Anatomica*, 155: 94-103.

Hayward S.W., Rosen M.A. & Cunha G.R. (1997). Stromal-epithelial interactions in the normal and neoplastic prostate. *British Journal of Urology*, 79: 18-26.

Knudson C.B. & Toole B.P. (1985). Changes in the pericellular matrix during differentiation of limb bud mesoderm. *Developmental Biololgy*, 112: 308-318.

Kofoed J.A., Tumilasci O.R., Curbelo H.M., Fernandez-Lemos S.M., Arias N.H. & Houssay A.B. (1990). Effects of castration and androgens upon prostatic proteoglycans in rats. *Prostate* 16: 93-102.

Kurita T., Cooke P.S. & Cunha G.R. (2001). Epithelial-stromal tissue interaction in paramesonephric (Mullerian) epithelial differentiation. *Developmental Biololgy*, 240: 194-211.

Lokeshwar V.B., Obek C., Soloway M.S. & Block N.L. (1997). Tumor-associated hyaluronic acid: a new sensitive and specific urine marker for bladder cancer. *Cancer Research* 57: 773-777.

Lokeshwar V. & Rubinowicz D. (1999). Hyaluronic acid and hyaluronidase: molecular markers associated with prostate cancer biology and detection. *Prostate Cancer Prostatic Disease*, 2(S3): S21.

Lokeshwar V.B., Rubinowicz D., Schroeder G.L., Forgacs E., Minna J.D., Block N.L., Nadji M. & Lokeshwar B.L. (2001). Stromal and epithelial expression of tumor markers hyaluronic acid and HYAL1 hyaluronidase in prostate cancer. *Journal of Biological Chemistry*, 276: 11922-32.

Owens G.K. (1995). Regulation of differentiation of vascular smooth muscle cells. *Physiology Review*,. 75: 487-517.

Rovner A.S., Murphy R.A. & Owens G.K. (1986). Expression of smooth muscle and nonmuscle myosin heavy chains in cultured vascular smooth muscle cells. *Journal of Biological Chemistry*, 261: 14741-14745.

Simpson M.A., Wilson C.M., Furcht L.T., Spicer A.P., Oegema T.R. & McCarthy J.B. (2002). Manipulation of hyaluronan synthase expression in prostate adenocarcinoma cells alters pericellular matrix retention and adhesion to bone marrow endothelial cells. *Journal of Biological Chemistry*, 277: 10050-10057.

Thomson A.A., Timms B.G. Barton L., Cunha G. R. & Grace O.C. (2002). The role of smooth muscle in regulating prostatic induction. *Development*, 129: 1905-1912.

Tuxhorn J.A., Ayala G.E. & Rowley D.R. (2001). Reactive stroma in prostate cancer progression. *Journal of Urology*, 166: 2472-2483.

Tuxhorn J.A., Ayala G.E., Smith M.J., Smith V.C., Dang T.D. & Rowley D.R. (2002). Reactive stroma in human prostate cancer: induction of myofibroblast phenotype and extracellular matrix remodeling. *Clinical of Cancer Research*, 8: 2912-2923.

Legends of the figures

Figure 1. Immunocytochemical identification of smooth muscle α-actin (**Fig. 1a**) and myosin heavy chain (**Fig. 1b**). The staining for myosin heavy chain is particulate and follows the general distribution of actin filaments in the cell. The cell nuclei were stained with DAPI.

Figure 2. Phalloidin staining of a rat prostate SMC in culture. The staining reveals a dense arrangement of stress fibers throughout the cytoplasm. The cell nucleus was stained with DAPI.

Figure 3. Expression of smoothelin (450 bp-visceral; 300 bp-vascular), calponin (125 bp) and SM22 (200 bp) by the rat prostatic SMC at the different passages. Expression of the three markers was observed throughout the experiments. β-actin (310 bp) expression was used as an internal standard to check cDNA quality and amount.

Figure 4. Expression of smoothelin, calponin and SM22 by the rat prostatic SMC cultured in the absence of any added hormone (N) and in presence of either testosterone (T) or insulin (I). Expression of the three markers was not modified by the presence or absence of testosterone or insulin. β-actin expression was used as an internal standard to check cDNA quality and amount.

Figure 5. HA concentration in the culture medium of rat prostatic SMC. The HA concentration in the culture medium showed a decrease up to passages 3 and 4, a sudden recover of the initial levels at passage 5 and a second decrease thereafter.

Figure 6. HA coat formation by SMC. Fig. 5a shows a micrograph with two selected cells in which the coat (red) and the cell (black) limits were highlighted. Fig. 5b is a dispersion diagram with the coat measurements. Values correspond to the ration between the total area (cell + coat) divided by the area of the cell. The values demonstrated that the cell coat did

virtually disappeared at passages 3 and 4, then recovering the wide variation observed at the beginning of the culture.

Figure 7. CD44 immunostaining of prostatic SMC. Staining was uniform at the cell surface of cells, and became more intense during cell division (Fig. 6a). In the presence of testosterone alone, CD44 staining accumulated at the cell periphery in one side of the cell (Fig. 6b).

Figure 1

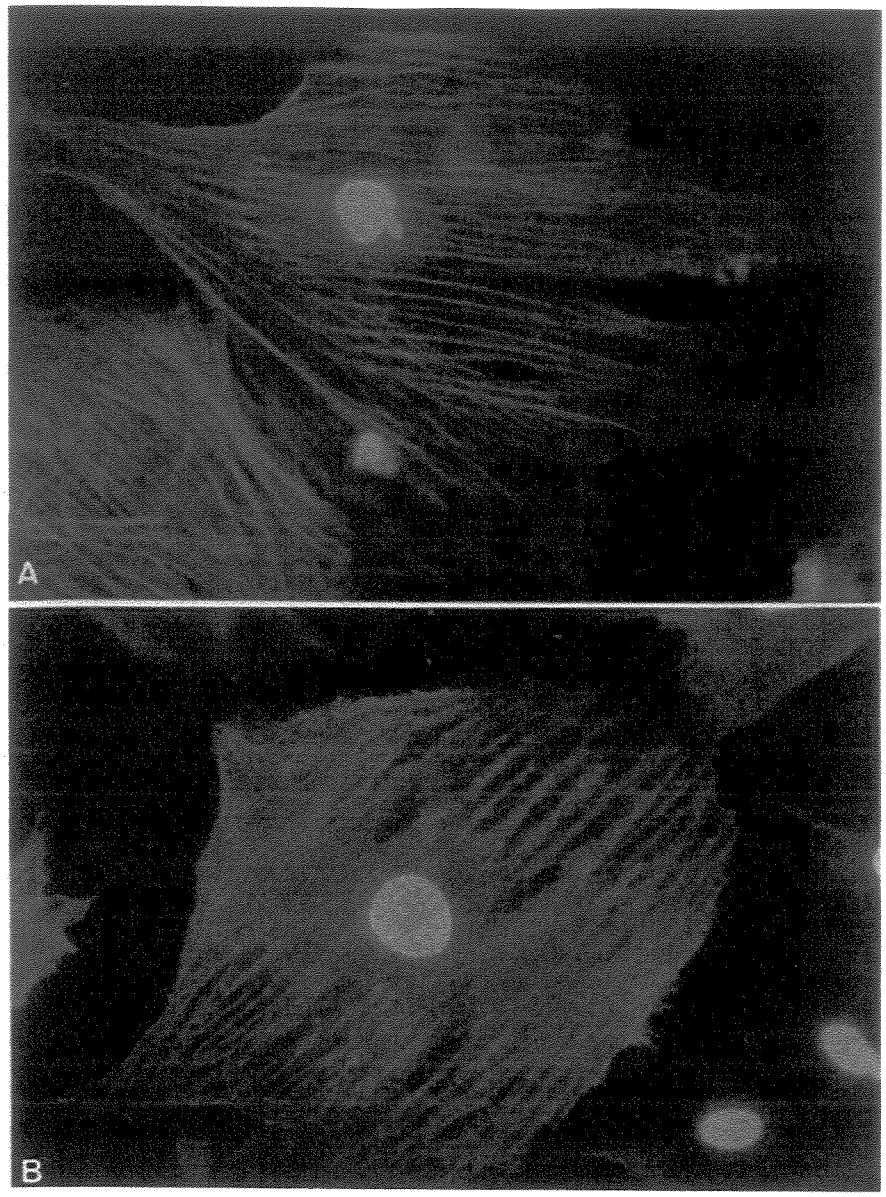

Figure 2

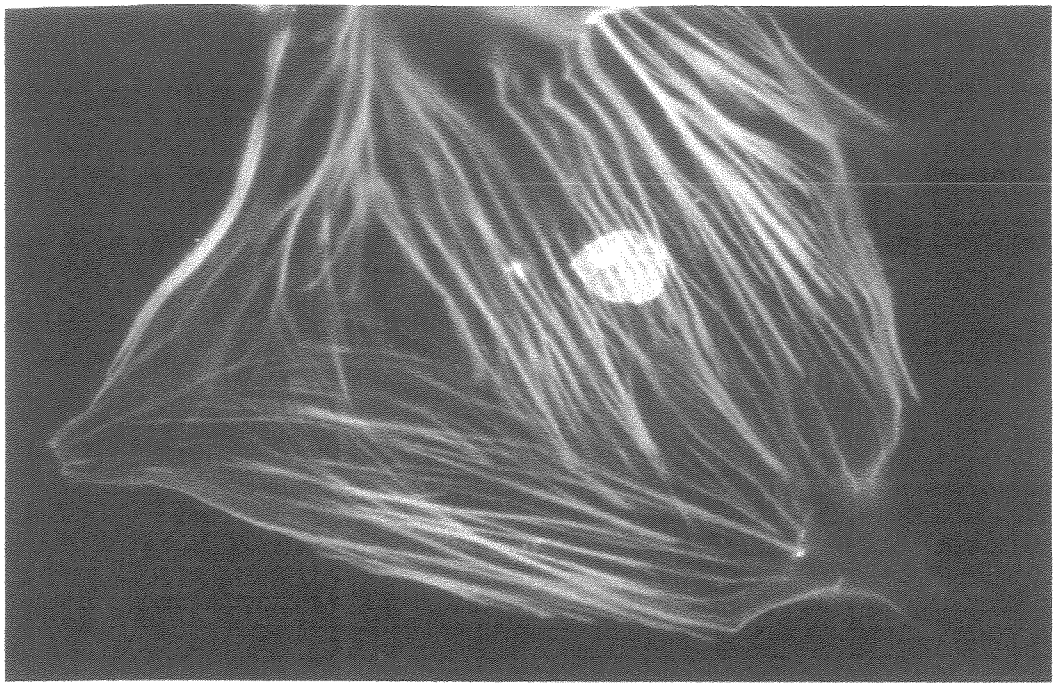

Figure 3

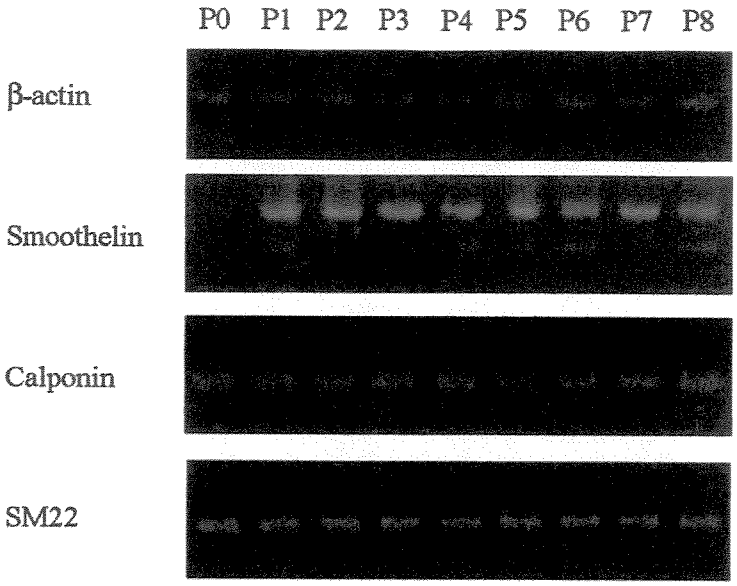

Figure 4

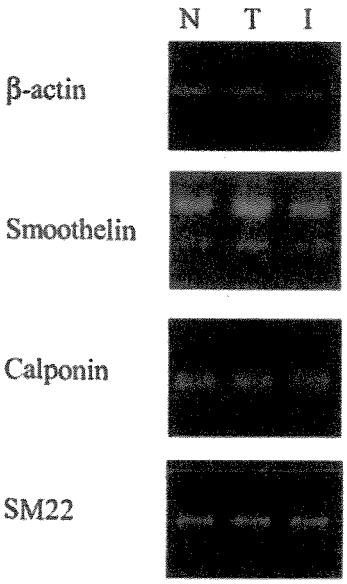

Figure 5

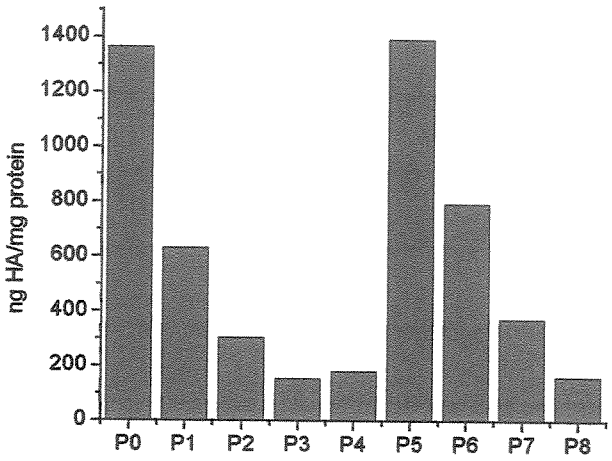

Figure 6

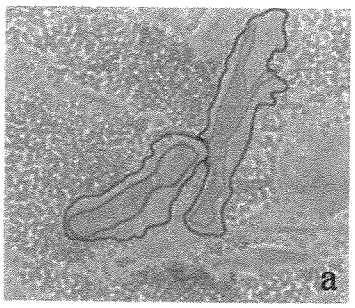

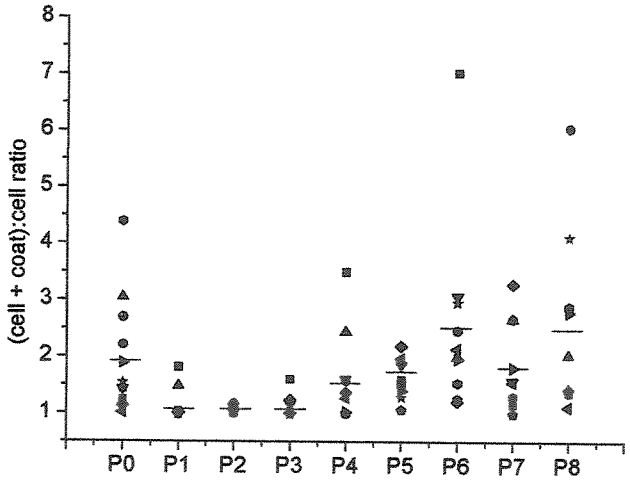

b

Figure 7

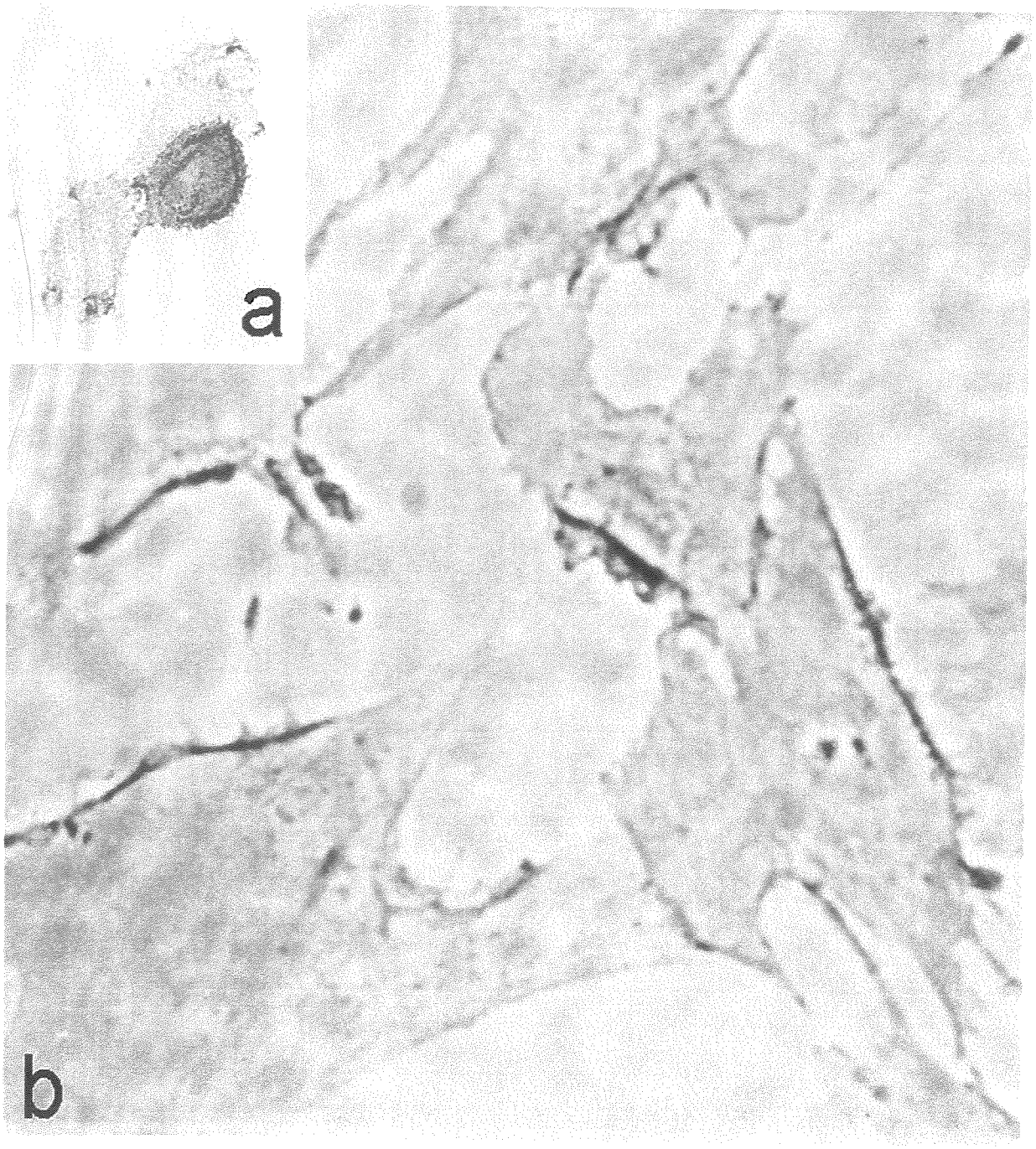

Conclusões Gerais

CONCLUSÕES GERAIS

1. O ácido hialurônico é encontrado tanto no compartimento epitelial, como no estroma, onde permanecem mesmo após a castração.
2. O conteúdo e o tamanho das cadeias de ácido hialurônico diminuem na próstata dos animais castrados, embora a sua concentração tecidual apareça aumentada.
3. O padrão apresentado pelas cadeias de ácido hialurônico na próstata dos animais castrados resulta da manutenção da expressão da HAS2, de um aumento na expressão da Hyal1 e de um decréscimo na atividade da hialuronidase lisossomal.
4. Os RNAm das enzimas HAS2 e Hyal1 foram encontrados tanto no epitélio quanto em diversas células estromais, sendo que suas expressões estão aparentemente aumentadas no estroma após a castração.
5. Células musculares lisas prostáticas preservam a expressão de pelo menos três marcadores do estado diferenciado quando mantidas em cultura mesmo após 8 passagens.
6. Nem insulina, nem testosterona foram capazes de modificar o padrão de expressão dos marcadores de células musculares lisas, num período de 96 h.
7. Células musculares lisas prostáticas sintetizam ácido hialurônico e o secretam para o meio de cultura e formam um *coat* na superfície celular.
8. Nas passagens 3 e 4 houve uma diminuição na síntese de AH, pelas células musculares lisas.

Referências Bibliográficas

REFERÊNCIAS BIBLIOGRÁFICAS

Antonioli E, Della Colleta HHM, Carvalho HF (2004) Smooth muscle cell behavior in the ventral prostate of castrated rats. J. Androl. 25: 50-56.

Berry SJ, Isaacs JT (1984) Comparative aspects of prostatic growth and androgen metabolism with aging in the dog versus the rat. Endocrinology 114: 511-20.

Brinck J, Heldin P (1999) Expression of recombinant hyaluronan synthase (HAS) isoforms in CHO cells reduces cell migration and cell surface CD44. Exp. Cell Res. 252: 342-351.

Camenisch TD, Spicer AP, Brehm-Gibson T, Biesterfeldt J, Augustine ML, Calabro A Jr, Kubalak S, Klewer SE, McDonald JA (2000) Disruption of hyaluronan synthase-2 abrogates normal cardiac morphogenesis and hyaluronan-mediated transformation of epithelium to mesenchyme. J. Clin. Invest. 106: 349-360.

Carvalho HF, Line SRP (1996) Basement membrane associated chances in the rat ventral prostate following castration. Cell Biol. Int. 20: 89-819.

Carvalho HF, Taboga SR, Vilamaior PSL (1997) Collagen type VI is a component of the extracellular matrix microfibrils network of the prostatic stroma. Tissue Cell 29: 163-170.

Cherr GN, Yudin AI, Overstreet JW (2001) The dual functions of GPI-anchored PH-20: hyaluronidase and intracellular signiling. Matrix Biol. 20: 515-525.

Corbier P, Martikainen P, Pestis J, Härkönen P (1995) Experimental research on the morphofunctional differentation of the rat ventral prostate: roles of the gonads at birth. Arch. Physiol. Biochem. 103: 699-714.

Comtesse N, Maldener E, Meese E (2001) Identificatio of a nuclear variant of MGEA5, a cytoplasmatic hyaluronidase and a beta-N-acetylglucosaminidase. Biochem. Biophys. Res. Commun. 283: 634-640.

Csóka AB, Scherer SW, Stern R (1999) Expression analysis of six paralogous human hyaluronidase genes clustered on chromosomes 3p21 and 7q31. Genomics 60: 356-361.

Csóka AB, Frost GI, Stern R (2001) The six hyaluronidase-like genes in the human and mouse genomes. Matrix Biol. 20: 499-508.

Cunha GR, Donjacour AA, Cooke PS, Mee S, Bigsby RM, Higgins SJ, Sugimura Y (1987) The endocrinology and developmental biology of the prostate. Endocr. Rev. 8: 338-362.

Cunha GR, Alarid ET, Turner T, Donjacour AA, Boutin EL, Foster BA (1992) Normal and abnormal development of the male urogenital tract. Role of androgens, mesenchymal-epithelial interactions, and growth factors. J. Androl. 13: 465-75.

De Salegui M, Pigman W (1967) The existence of an acid-active hyaluronidase in serum. Arch. Biochem. Biophys. 120: 60-67.

Donjacour AA, Cunha GR (1988) The effect of androgen deprivation on branching morphogenesis in the mouse prostate. Dev. Biol. 128: 1-14.

Dorfman A, Ott ML, Whitney R (1948) The hyaluronidase inhibitor of human blood. J. Biol. Chem. 174: 621-629.

Farnsworth WE (1999) Prostate stroma: Physiology. Prostate. 38: 60-72.

Flannery CR, Little CB, Hughes CE, Caterson B (1998) Expression and activity of articular cartilage hyaluronidases. Biochem. Biophys. Res. Commun. 251: 824-829.

Fiszer-Szafarz B (1968) Demonstration of a new hyaluronidase inhibitor in serum of cancer patients. Proc. Soc. Exp. Biol. Med. 129: 300-302.

Frost GI, Csóka TB, Wong T, Stern R (1997) Purification, cloning and expression of human plasma hyaluronidase. Biochem. Biophys. Res. Commun. 236: 10-15.

Gakunga P, Frost G, Shuster S, Cunha G, Formby B, Stern R (1997) Hyaluronan is a prerequisite for ductal branching morphogenesis. Development 124: 3987-3997.

Gold EW (1982) Purification and properties of hyaluronidase from human liver. Differences from and similarities to the testicular enzyme. Biochem. J. 205: 69-74.

Haas E (1946) On the mechanism of invasion .1. antinvasin-I, an enzyme in plasma. J. Bio. Chem.163: 63-88.

Hascall VC, Laurent TV (1997) Hyaluronan: structure and physical properties. Glycoforum, (http://www.glycoforum.gr.jp/science/hyaluronan/HA01/HA01E.html).

Hayward SW, Haughney PC, Rosen MA, Greulich KM, Weier HU, Dahiya R, Cunha GR (1998) Interactions between adult human prostatic epithelium and rat urogenital sinus mesenchyme in a tissue recombination model. Differentiation 63: 131-40.

Hayward SW, Cunha GR (2000) The prostate: Development and physiology. Radiologic Clinics of North America. 38: 1-14.

Heckel D, Comtesse N, Brass N, Blin N, Zang KD, Meese E (1998) Novel immunogenic antigen homologous to hyaluronidase in meningioma. Hum. Mol. Genet. 7: 1859-1872.

Heldermon C, De Angelis P, Weigel PH (2001) Topological organization of the hyaluronan synthase from *Streptococcus pyogenes*. J. Bio. Chem. 276: 2037-2046.

Husmann LK, Yung DL, Hollingshead SK, Scott JR (1997) Role of putative virulence factors of *Streptococcus pyogenes* in mouse models of long-term throat colonization and pneumonia. Infect. Immun. 65: 1422-1430.

Ichikawa T, Itano N, Sawai T, Kimata K, Koganehira Y Saida T, Taniguchi S (1999) Increased synthesis of hyaluronate enhances motility of human melanoma cells. J. Invest. Dermatol. 113: 935-939.

Ilio KY, Nemeth JA, Sensibar JA, Lang S, Lee C (2000) Prostatic ductal system in rats: changes in regional distribution of extracellular matrix proteins during castration-induced regression. Prostate 43: 3-10.

Itano N, Sawai T, Yoshida M, Lenas P, Yamada Y, Imagawa M, Shinomura T, Hamaguchi M, Yoshida Y, Ohnuki Y, Miyauchi S, Spicer AP, McDonald JA, Kimata K (1999a) Three isoforms of mammalian hyaluronan synthases have distinct enzymatic properties. J. Biol. Chem. 274: 25085-25092.

Itano N, Sawai T, Miyaishi O, Kimata K (1999b) Relationship between hyaluronan production and metastatic potential of mouse mammary carcinoma cells. Cancer Res. 59: 2499-2504.

Itano N, Atsumi F, Sawai T, Yamada Y, Miyaishi O, Senga T, Hamaguchi M, Kimata K (2002) Abnormal accumulation of hyaluronan matrix diminishes contact inhibition of cell growth and promotes cell migration. Proc. Natl. Acad. Sci. USA 99: 3609-3614.

Jacobson A, Brinck J, Briskin MJ, Spicer AP, Heldin P (2000) Expression of human hyaluronan synthases in response to external stimuli. Biochem. J. 348: 29-35.

Knox JD, Cress AE, Clark V, Monriquez L, Affinito K-S, Dalkin BL, Nagle RB (1994) Differential expression of extracellular matrix molecules and the alpha 6-integrins in the normal and neoplastic prostate. Am. J. Pathol. 145: 167-174.

Kofoed JA, Tumilasci OR, Curbelo HM, Fernandez Lemos SM, Arias NH, Houssay AB (1990) Effects of castration and androgens upon prostatic proteoglycans in rats. Prostate 16: 93-102.

Koprunner M, Mullegger J, Lepperdinger G (2000) Synthesis of hyaluronan of distinctly different chain lenght is regulated by differential expression of Xhas 1 and 2 during early development of *Xenopus laevis*. Mech. Dev. 90: 275-278.

Kosaki R, Watanabe K, Yamaguchi Y (1999) Overproduction of hyaluronan by expression of the hyaluronan synthase Has2 enhances anchorage-independent growth and tumorigenicity. Cancer Res. 59: 1141-1145.

Kurita T, Wang YZ, Donjacour AA, Zhao C, Lydon JP, O'Malley BW, Isaacs JT, Dahiya R, Cunha GR (2001) Paracrine regulation of apoptosis by steroid hormones in the male and female reproductive system. Cell Death Differ. 8: 192-200.

Labat-Robert J, Bihari-Varga M, Robert L (1990) Extracellular matrix. FEBS Lett. 268: 368-393.

Laurent TC, Laurent UB, Frase JR (1996) The structure and function of hyaluronan: An overview. Immunol. Cell Biol. 74: A1-7.

Lee C, Sensibar JA, Dudek SM, Hiipakka RA, Liao S (1990) Prostatic ductal system in rats: Regional variation in morphological and functional activities. Biol. Reprod. 43: 1079-1086.

Lee C (1996) Role of androgen in prostate growth and regression: stromal-epithelial interaction. Prostate 6: 52-56.

Liu N, Lapcevich RK, Underhill CB, Han Z, Gao F, Swartz G, Plum SM, Zhang L, Gree SJ (2001) Metastatin: a hyaluronan-binding complex from cartilage that inhibits tumor growth. Cancer Res. 61: 1022-1028.

Lin Y, Mahan K, Lathrop WF, Myles DG, Primakoff P (1994) A hyaluronidase activity of the sperm plasma membrane protein PH-20 enables sperm to penetrate the cumulus cell layer surrounding the egg. J. Cell. Biol., 125: 1157-1163.

Mathews MB, Dorfman A (1955) Inhibition of hyaluronidase. Physiol. Rev. 35: 381-402.

Meyer K, Palmer JW (1934) The polysaccharide of the vitreous humor. J. Biol. Chem. 107: 629-634.

Meyer K (1950) The action of hyaluronidases on hyaluronic acid. Ann N Y Acad Sci. 52: 1021-3.

Mio K, Carrette O, Maibach HI, Stern R (2000) Evidence that the serum inhibitor of hyaluronidase may be a member of the inter-α-inhibitor family. J. Biol. Chem., 275: 32413-32421.

Mio K, Stern R (2002) Inhibitors of the hyaluronidases. Matrix Biol. 21: 31-37.

Moore DH, Harris TN (1949) Occurrence of hyaluronidase inhibitors in fractions of electrophoretically separated serum. J. Biol. Chem. 179: 377-381.

Nemeth H, Lee C (1996) Prostatic dutal system in rats: Regional variation in stromal organization. Prostate 28: 124-128.

Newman JK, Berenson GS, Mathews MB, Goldwasswer E, Dorfman A (1955) The isolation of the non-specific hyaluronidase inhibitor of human blood. J. Biol. Chem. 217: 31-41.

Noble PW (2002) Hyaluronan and its catabolic products in tissue injury and repair. Matrix Biol. 21: 25-9.

Ouskova G, Spellerberg B, Prehm P (2004) Hyaluronan release from *Streptococcus pyogenes*: export by an ABC transporter. Glycobiology 14: 931-938.

Pointis G, Latreille MT, Cedard L (1980) Gonado-pituitary relationships in the fetal mouse at various times during sexual differentiation. J. Endocrinol. 86: 483-488.

Prehm P (1984) Hyaluronate is synthesized at plasma membranes. Biochem J. 220: 597-600.

Prehm P, Schumacher U (2004) Inhibition of hyaluronan export from human fibroblast by inhibitors of multidrug resistence transporters. Biochem. Pharmacol. 68: 1401-1410.

Primakoff P, Hyatt H, Myles DG (1985) A role for the migrating sperm surface antigen PH-20 in guinea pig sperm binding to the egg zona pellucida. J. Cell. Biol. 101: 2239-2244.

Prins GS, Birch L, Greene GL (1992) Androgen receptor localization in different cell types of the adult rat prostate. Endocrinology 129: 3187-3199.

Rosa F, Sargent TD, Rebbert ML, Michaels GS, Jamrich M, Grunz H, Jonas E, Winkles JA, Dawid IB (1988) Accumulation and decay of DG42 gene products follow a gradient pattern during *Xenopus* embryogenesis. Dev Biol 129: 114-123.

Sayo T, Sugiyama Y, Takahashi Y, Ozawa N, Sakai S, Ishikawa O, Tamura M, Inoue S (2002) Hyaluronan synthase 3 regulates hyaluronan synthesis in cultured human keratinocytes. J. Invest. Dermatol. 118: 43-48.

Shabsigh A, Tanji N, D'agati V, Burchardt T, Burchardt M, Hayek O, Shabsigh R, Buttyan R (1999) Vascular anatomy of the rat ventral prostate. Anat. Rec. 256: 403-411.

Shapiro E, Hartanto V, Becich MJ, Lepor H (1992) The relative proportion of stromal and epithelial hyperplasia is related to the development of symptomatic BPH. J. Urol. 147: 1293-1297.

Shyjan AM, Heldin P, Butcher EC, Yoshino T, Briskin MJ (1996) Functional cloning of the cDNA for a human hyaluronan synthase. J. Biol. Chem. 271: 23395-23399.

Spicer AP, Olson JS, McDonald JA (1997) Molecular cloning and characterization of a cDNA encoding the third putative mammalian hyaluronan synthase. J. Biol. Chem. 272: 8957-8961.

Spicer AP, McDonald JA (1998) Characterization and molecular evolution of a vertebrate hyaluronan synthase gene family. J. Biol. Chem. 273: 1923-1932.

Stern R, Csóka AB (2000) Mammalian hyaluronidases. Glycoforum, (http://www.glycoforum.gr.jp/science/hyaluronan/HA15/HA15E.html).

Stern R (2003) Devising a pathway for hyaluronan catabolism: are we there yet? Glycobiology 13: 105R-115R.

Sugimura Y, Cunha GR, Donjacour AA (1986) Morphogenesis of dutal networks in the mouse prostate. Biol. Reprod. 34: 961-971.

Takeda I, Lasnitzki I, Mizuno T (1986) Analysis of prostatic bud induction by brief androgen treatment in the fetal rat urogenital sinus. J. Endocrinol. 110: 467-470.

Tammi R. Rilla K, Pienimaki JP, MacCallum DK, Hogg M, Luukkonen M, Hascall VC, Tammi M (2001) Hyaluronan enters keratinocytes by a novel endocytic route for catabolism. J. Biol. Chem. 276: 35111-35122.

Tammi MI, Day AJ, Turley EA (2002) Hyaluronan and homeostasis: a balancing act. J. Biol. Chem. 277: 4581-4584.

Taplin ME, e Ho S-M (2001) The endocrinology of the prostate cancer. J. Clin. Endocrinol. Metabol. 86: 3467-3477.

Tlapak-Simmons VL, Kempner ES, Baggenstoss BA, Weigel PH (1998) The active streptococcal hyaluronan synthases (HASs) contain a single HAS monomer and multiple cardiolipin molecules. J. Biol. Chem. 273: 26100-26109.

Tlapak-Simmons VL, Baggenstoss BA, Clyne, T, Weigel PH (1999a) Purification and lipid dependence of the recombinat hyaluronan synthases from *Streptococcus pyogenes* and *Streptococcus equisimilis*. J. Biol. Chem. 274: 4239-4245.

Tlapak-Simmons VL, Baggenstoss BA, Kumari K, Heldermon C, Weigel PH (1999b) Kinetic characterization of the recombinant hyaluronan synthases from *Streptococcus pyogenes* and *Streptococcus equisimilis*. J. Biol. Chem. 274: 4246-4253.

Thomson AA, Timms BG, Barton L, Cunha GR, Grace OC (2002) The role of smooth muscle in regulating prostatic induction. Development 129:1905-1912.

Timms TL, Truong LD, Merz VW, Krebs T, Kadmon D, Flanders KC, Park SH, Thompson TC (1994) Mesenquimal-epithelial interactions and transforming growth factor-β expression during mouse prostate morphogenesis. Endocrinology 134:1039-1045.

Toole BP, Wight TN, Tamii MI (2002). Hyaluronan-cell interactions in cancer and vascular disease. J. Biol. Chem. 277: 4593-4596.

Toole BP (2004) Hyaluronan: from extracellular glue to pericellular cue. Nature Rev. 4: 528-539.

Turley EA, Noble PW, Bourguignon LY (2002) Signaling properties of hyaluronan receptors. J. Biol. Chem. 277: 4589-4592.

Vilamaior PSL, Felisbino SL, Taboga SR, Carvalho HF (2000) Collagen fiber reorganization in the rat ventral prostate following androgen deprivation: a possible role for the smooth muscle cells. Prostate 45: 253-258.

Walden PD, Lefkowitz GK, Ficazzola M, Gitlin J, Lepor H (1998) Identification of genes associated with stromal hyperplasia and glandular atrophy of the prostate by mRNA differential display. Exp. Cell. Res. 245: 19-26.

Watanabe K, Yamaguchi Y (1996) Molecular identification of a putative human hyaluronan synthase. J. Biol. Chem. 271: 22945-22948.

Weigel, PH, Hascall VC, Tammi M (1997) Hyaluronan synthases. J. Biol. Chem. 272: 13997-14000.

Weissman B, Meyer K (1954) The structure of hyalobiuronic acid and of hyaluronic acid from umbilical cord. J. Am. Chem. Soc. 76: 1753-1747.

Wessels MR, Moses AE, Goldberg JB, DiCesare TJ (1991) Hyaluronic acid capsule is a virulence factor for mucoid group A streptococci. Proc. Natl. Acad. Sci. USA 88: 8317-8321.

Zimmerman E, Geiger B, Addadi L (2002) Initial stages of cell-matrix adhesion can be mediated and modulated by cell-surface hyaluronan. Biophys. J. 82: 1848-1857.